

# The Effects of Different Urban Street Networks on their Ability to Recover from Congestion

**Nicolas Mühlich**

Supervisors:

Dr. Vikash V. Gayah (The Pennsylvania State University)

Dr. Monica Menendez (ETH Zürich)

**Masterthesis Spatial Development and Infrastructure Systems**

**Institute for Transport Planning and Systems**

**July 2014**



Eidgenössische Technische Hochschule Zürich  
Swiss Federal Institute of Technology Zurich

## **Acknowledgement**

First of all I would like to thank Dr. Vikash Gayah for his support, guidance and valuable comments and for enabling me to write my master thesis at the Pennsylvania State University in State College. Thanks to Dr. Monika Menendez, my supervisor at the ETH Zurich for making this semester in the United States possible in the first place and for her valuable inputs in the process of this thesis. I also want to thank Anne-Kathrin Bodenbender, whose advice regarding her experience as a graduate student in the United States helped me greatly in arranging my stay in State College.

Thank you to Javier Ortigosa, Jeff Gooch and Andy Nagle for their valuable input and to Alaina Symanovich for proofreading.

I am very grateful for the financial contribution of the Swiss-American Society and the Philip Degen Foundation at the ETH Zurich for my stay abroad.

I also would like to thank all the people here in State College who contributed in one way or another to four great months. Special thanks go to my fellow students and friends at the ETH for two wonderful years during our master program with memories that will last a lifetime.

Last but not least, I want to thank my family, especially my mother, Ruth, for supporting me throughout my entire schooling.

# Contents

<b>1</b>	<b>Introduction</b>	<b>1</b>
1.1	MFD and the formation of hysteresis loops . . . . .	4
1.2	Properties of urban networks . . . . .	7
1.3	Objective of this master thesis . . . . .	10
<b>2</b>	<b>Methodology</b>	<b>11</b>
2.1	Methodology . . . . .	11
2.2	Micro simulation . . . . .	11
2.3	Patterns, intersection layout and signal phases . . . . .	12
2.4	Demand and routing . . . . .	15
2.5	Adaptive driving . . . . .	16
<b>3</b>	<b>Results</b>	<b>19</b>
3.1	Comparison within a specific pattern . . . . .	20
3.2	Comparison among different patterns . . . . .	26
3.3	Impact of heterogeneity on traffic performance . . . . .	28
3.4	Spatial distribution of congestion . . . . .	30
3.5	Arterial streets . . . . .	32
3.6	Local feeder streets . . . . .	33
3.7	Turning maneuvers . . . . .	36
<b>4</b>	<b>Discussion</b>	<b>39</b>
4.1	Limitations and assumptions . . . . .	39
4.2	Main findings . . . . .	40
4.3	Practical significance . . . . .	41
4.4	Remaining questions for further research . . . . .	42
<b>5</b>	<b>Conclusion</b>	<b>43</b>
<b>6</b>	<b>References</b>	<b>44</b>
<b>A</b>	<b>Selection of urban network patterns</b>	<b>46</b>

## List of Figures

1	Fundamental diagram . . . . .	2
2	Clockwise hysteresis loops . . . . .	3
3	MFD for Yokohama and Toulouse . . . . .	5
4	MFD for different levels of adaptive driving . . . . .	6
5	Street network design . . . . .	7
6	Components of a street network . . . . .	9
7	Network screenshot from Aimsun . . . . .	12
8	Implemented patterns . . . . .	13
9	Intersection layouts, signal phases and cycle lengths . . . . .	15
10	Adaptive driving . . . . .	17
11	Different levels of adaptivity . . . . .	18
12	Flow-density plot of pattern 3 . . . . .	20
13	Time-space plot of pattern 1 . . . . .	21
14	Time-space plot of pattern 2 . . . . .	22
15	Time-space plot of pattern 3 . . . . .	23
16	Time-space plot of pattern 4 . . . . .	24
17	Time-space plot of pattern 5 . . . . .	25
18	Time-space plot for all patterns . . . . .	27
19	Mean link density vs. variance of link density . . . . .	29
20	Spatial distribution of congestion for all A versions . . . . .	30
21	Spatial distribution of congestion for patterns 2 and 4 . . . . .	31
22	Ratio of arterial street density to local street density . . . . .	32
23	Street types of pattern 2 . . . . .	33
24	Mean link density for A versions . . . . .	34
25	Mean link density for B versions . . . . .	35
26	Total maneuvers at intersections . . . . .	38
27	Selection of urban network patterns . . . . .	46

## **List of Tables**

1	Network length of the explored patterns . . . . .	13
2	Fractions of the network length for all A versions . . . . .	35
3	Fractions of the network length for all A versions . . . . .	36
4	Turning maneuvers at intersections . . . . .	37

Masterthesis Spatial Development and Infrastructure Systems

# **The Effects of Different Urban Street Networks on their Ability to Recover from Congestion**

Nicolas Mühlich,  
Schwylerstrasse 7  
CH-8712 Stäfa

phone: +41 79 616 93 87

mnicolas@student.ethz.ch

July 2014

## **Abstract**

Five different idealized networks were constructed and evaluated for this thesis using micro simulation. Each network consists of a local street network and an arterial street network, which represent the micro and macro structure of an urban network. It was confirmed that networks are inherently more unstable as they recover from congestion than during its onset, resulting in the formation of hysteresis loops behavior in macroscopic relationships between urban traffic measures. This thesis examines one such relationship - the Macroscopic Fundamental Diagram (MFD) - and uses the size and shape of these hysteresis loops to explore and quantify the effects of different network patterns on the network's ability to recover from congested conditions. The patterns produced different MFDs and hysteresis loops of varying shape and size. It can be observed that the spatial distribution of congestion differs between the explored patterns. Networks with a more heterogeneous distribution of congestion were found to lack a well-defined MFD. The amount and placement of arterials and local streets feeding the arterials seemed to create a more heterogeneous traffic distribution for some of the networks than for others. The network structure also influences the number of turning maneuvers, which were found to have a relationship with network performance as well. Fewer turning maneuvers and more through movements at intersections were associated with better network performance, i.e. less hysteresis and greater network productivity.

## **Keywords**

street networks, urban patterns, congestion, Macroscopic Fundamental Diagram, hysteresis loop

## **Preferred citation style**

Mühlich, N. (2014) The Effects of Different Urban Street Networks on their Ability to Recover from Congestion, *Masterthesis Spatial Development and Infrastructure Systems*, Institute for Transport Planning and Systems, ETH Zurich, Zurich.

Masterarbeit Raumentwicklung und Infrastruktursysteme

# The Effects of Different Urban Street Networks on their Ability to Recover from Congestion

Nicolas Mühlich,  
Schwylerstrasse 7  
CH-8712 Stäfa

Tel: +41 79 616 93 87

mnicolas@student.ethz.ch

Juli 2014

## Zusammenfassung

Im Rahmen dieser Arbeit wurden fünf unterschiedliche idealisierte Strassennetze in einer Mikrosimulation erstellt und evaluiert. Jedes Strassennetz ist aus Erschliessungs- und Verbindungsstrassen aufgebaut, welche die Mikro- und Makrostruktur eines urbanen Strassennetzes immitieren. Es wurde bestätigt, dass sich Netzwerke nach einer Stauperiode instabiler verhalten als während der Staubiildung, was zur Bildung von Hysteresekurven führt. Anhand des makroskopischen Fundamentaldiagramms (MFD) und aufgrund der Grösse und der Form der Hysteresekurven wurden die Effekte der unterschiedlichen Strassennetze hinsichtlich ihrer Leistungsfähigkeit und ihrem Erholungsvermögen von Stausituationen untersucht. Es wurde festgestellt, dass die räumliche Stauverteilung zwischen den unterschiedlichen Strassennetzen variiert. Strassennetze mit einer homogeneren Verkehrsverteilung weisen kein klar definiertes MFD auf. Die Anzahl und Platzierung der Verbindungsstrassen beeinflusst die Homogenität der einzelnen Netzwerke. Nebst den Verbindungsstrassen scheinen auch die Zuflussstrassen auf die Verbindungsstrassen einen erheblichen Einfluss auf die räumliche Stauverteilung und somit auch auf die Leistungsfähigkeit des ganzen Strassennetzes zu haben. Die Netzwerkstruktur wirkt sich auch auf die Abbiegebeziehungen aus. Weniger Abbiegemanöver und ein höherer Anteil an Geradeausfahrten führen zu einer höheren Leistungsfähigkeit, d.h. weniger Hysterese und eine höhere Netzwerk Produktivität.

## Schlüsselwörter

Strassennetz, Stadtstruktur, Stau, Makroskopisches Fundamentaldiagramm, Hysteresekurve

## Bevorzugter Zitierstil

Mühlich, N. (2014) The Effects of Different Urban Street Networks on their Ability to Recover from Congestion, *Masterarbeit Raumentwicklung und Infrastruktursysteme*, Institut für Verkehrsplanung und Transportsysteme, ETH Zürich, Zürich.

# **1 Introduction**

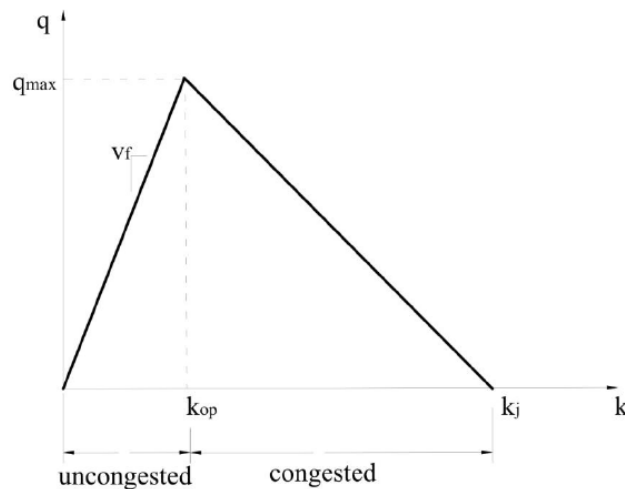
Transportation is essential for the development and growth of modern societies. The worldwide increase in population, wealth and vehicle ownership has increased the need and desire for people to move themselves and their goods from one place to another, resulting in the construction of vast transportation systems. However, the benefits of improved transportation come not without costs. Transportation creates noise, changes the environment, pollutes air, costs money and consumes a considerable portion of society's time and resources.

In the past, increasing demand in the transportation sector has often been met by building new infrastructure or increasing the capacity of existing infrastructure. However, the provision of more supply often does not satisfy people's need and desire to move from one place to another, but actually generates even more demand. This phenomenon is known as induced demand (Cervero, 2002). For this reason, instead of expanding transportation systems, improving traffic management strategies, and using existing infrastructure more efficiently, are becoming more important. These new developments are particularly needed in urban areas. For the first time in history, more than half of the world's population lives in cities (Martine and Alex, 2007). The concentration of people, jobs, activities and leisure possibilities, combined with the limited amount of space, exacerbates the negative effects of transportation in urban areas and often leads to heavily congested areas.

In order to develop strategies that can tackle the challenges of transportation in modern cities, it is necessary to understand how traffic forms in cities. One factor that determines urban traffic is the structure of a city, i.e., its urban pattern. On one hand, urban structure and land use determines the amount and placement of transportation facilities, such as streets, parking lots, sidewalks or railway infrastructure. On the other hand, transportation infrastructure has also formed urban structure and generated settlement growth to an extent that some cities could also be described as products of their transport system (Marshall, 2013). Clearly, a strong relationship exists between transportation and urban structure. This thesis explores and attempts to understand this relationship through a comparison of the network traffic performance of different idealized urban patterns.

The tool that will be used throughout this thesis as an indicator for the performance of traffic on urban street network is known as the Macroscopic Fundamental Diagram (MFD). The MFD can be regarded as the aggregated network version of the fundamental diagram, a well-known relationship that is used to model traffic behavior at the individual link level, illustrated in Fig. 1.

Figure 1: Fundamental diagram



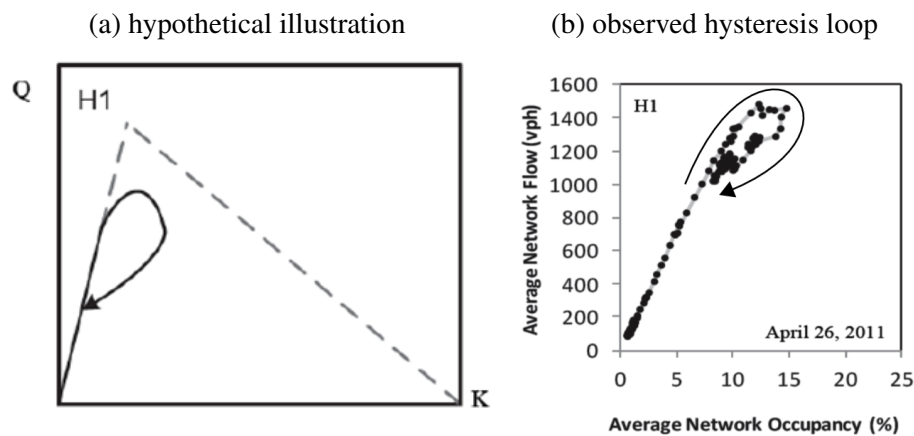
Source: Menendez (2014)

Although other traffic properties may be used in some cases, it is customary to use the relationship between flow,  $q$  (measured in vehicles per unit of time), and density,  $k$  (measured in vehicles per unit of distance). The fundamental diagram (or  $q$ - $k$  diagram) can be used to describe the traffic movement along a road, such as a highway. The left branch of the diagram describes traffic in uncongested conditions with all vehicles presumed to drive with free-flow speed  $v_f$ , the ratio of flow to density. The right branch of the fundamental diagram describes traffic in congested or queued condition with vehicles driving at a speed smaller than  $v_f$ . The maximum flow, i.e., the capacity of the highway, is denoted as  $q_{max}$  and is reached at an optimal density,  $k_{opt}$ . If density increases and the traffic state is already on the congested branch of the fundamental diagram, flow will decrease until the traffic completely jams at a jam density,  $k_j$ .

The MFD expresses the same relationship of flow, density and speed, but instead of describing a single link, it describes an entire urban street network or a portion of a network (i.e., a small neighborhood). Therefore, an MFD presents a relationship between the weighted average of flow and density measured on all links within the area of interest, using the length of each link as the weight. The ratio of the average network flow to the average network density is the average network speed. In networks with a well-defined MFD, the average flow and density is related by a unique and reproducible curve.

It has been observed that in reality, the shape of the MFD is not always well-defined (Buisson and Ladier (2009), Geroliminis and Sun (2011)). For higher densities, the value points often scatter and multiple flow states are observed. If an interpolated line is used to connect each pair of temporally consecutive points on the MFD, the resulting scatter follows a hysteretic pattern, resulting in the formation of a clockwise hysteresis loop. Figure 2 shows a hypothetical illustration as well as an observed hysteresis loop from a real-world network to illustrate this phenomenon.

Figure 2: Clockwise hysteresis loops



Source: Saberi and Mahmassani (2013)

The abscissa of the MFD represents the average network density, respectively the average network occupancy, which can be regarded as a proxy for the network density,  $k$ . It is observable that density is increasing until a certain value. This stage can be describe as the ‘loading phase’, suggesting that the traffic in a network is increasing. For example, during the start of a rush hour, which results in a partly congested urban network. After the maximum density has been reached, density would start to decrease again, as would be the case at the end of a rush hour when the congested areas start to dissolve. This stage can then be described as the ‘recovery phase’. By looking at the flow, shown on the ordinate of the MFD, it can be noted that due to the existence of a hysteresis loop, for the same value of average network density, the average network flow is lower during the recovery phase compared to the loading phase.

It has been found that the formation of such hysteresis loops arises even under the most favorable conditions for an MFD (Gayah and Daganzo, 2011a) and they have also been observed in empirical data (Buisson and Ladier (2009), Geroliminis and Sun (2011)). However, the shape and size of the hysteresis loops for different networks differ greatly and reflect the level of instability of traffic and the efficiency of the recovery phase compared to the loading phase. Networks with a small hysteresis loop can recover more quickly from congested conditions than networks with a large hysteresis loop. Furthermore, smaller hysteresis loops are beneficial as

they indicate a more predictable behavior during congestion recovery. Therefore, the MFD can be used as an indicator for the overall traffic performance of a network, and the existence and size of the hysteresis loop can reveal insights about the ability of a network to recover from congested conditions.

Section 1.1 provides additional background information about the MFD and the formation of hysteresis loops. Section 1.2 shows some examples of urban networks, explains their properties and introduces an integrated framework in order to facilitate the characterization of street networks. Finally, Section 1.3 describes the research question and provides the organization of the rest of this thesis.

## **1.1 MFD and the formation of hysteresis loops**

Initial efforts to describe traffic movement in urban networks on an aggregate level have been made by Godfrey (1969), who proposed the existence of an MFD as a unimodal relationship between average flow and average density in a network. Herman and Prigogine (1979) reintroduced this idea as a refinement to their two-fluid model. However, the data used in these early studies mostly came from lightly congested real-world networks or from simulations and were too sparse or not investigated deeply enough to demonstrate that an invariant MFD could dynamically arise in the real world.

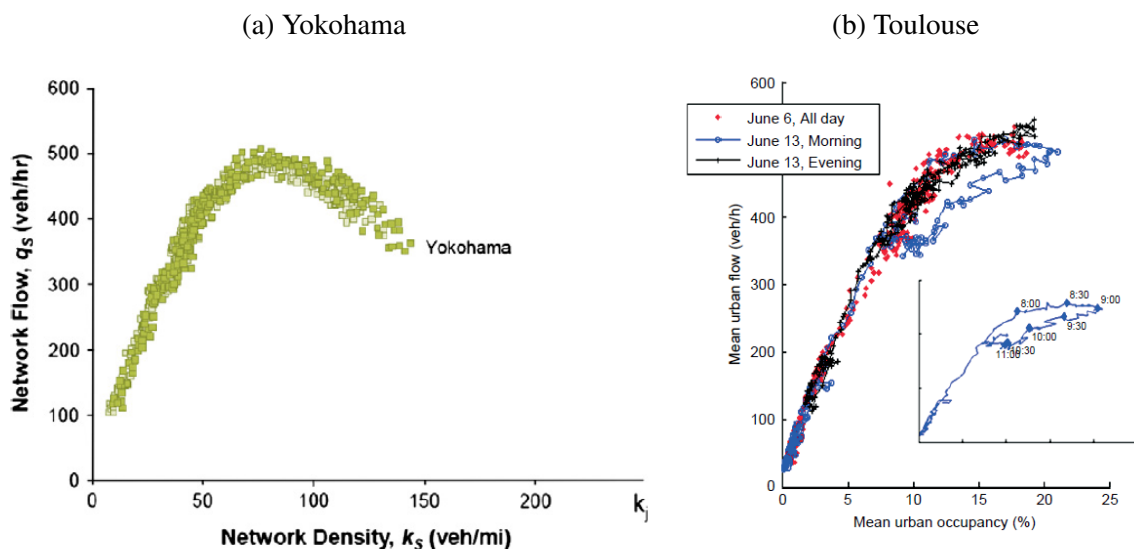
Daganzo (2007) appears to be the first to introduce the idea of monitoring and controlling aggregate vehicular accumulations at the ‘neighborhood’ level, i.e., areas within a city that are relatively homogeneous, to improve urban mobility. He proposed a macroscopic relationship between total outflow from the system and the aggregate accumulation for a single system. Geroliminis and Daganzo (2007) conjectured that under certain conditions the production of a network is the sum of the measures for individual links and can be expressed as a function of the total accumulation of the network independently of the disaggregate link data. Using simulations for two arterial test sites, the authors verified the existence of an MFD linking space-mean flow, density and speed, as proposed by Godfrey (1969).

This finding was confirmed by the same authors in another study through a field experiment in Yokohama, Japan combining fixed detectors and GPS equipped taxis as floating vehicle probes (Geroliminis and Daganzo, 2008). The authors observed that points on an aggregated scatter plot of speed vs. density grouped neatly along a smoothly declining curve, as shown in Fig. 3(a). The network was assumed to be homogeneous in regards to congestion. As a result of this finding, the authors conjectured that large urban areas in general should have a well-defined MFD, independent of demand. The authors also revealed a fixed relationship between space-mean

flows on the whole network and the trip completion rates.

Buisson and Ladier (2009) delved further into this subject by exploring the existence of an MFD for the surface street and freeway network of the city of Toulouse, France. For one day, the authors observed the absence of a well-defined MFD. On the morning of June 13, for a range of occupancies multiple flows were observed. If the observed value pairs for this day are connected through an interpolated line, a hysteresis loop can be observed. As the time stamps in the specific analysis of the hysteresis loop in Fig. 3(b) show, the formation of the loop is clockwise, i.e., the network carries higher flows for the same mean urban occupancy as the mean occupancy increases and lower flows as the mean occupancy decreases. The authors related the formation of a clockwise hysteresis loop to a heterogeneous evolution of congestion during that day due to a strike movement of truck drivers on a freeway section. Buisson and Ladier (2009) concluded that heterogeneity in a network has a strong impact on the shape of the MFD, thereby questioning the homogeneity assumption made by Geroliminis and Daganzo (2008).

Figure 3: MFD for Yokohama, Japan and Toulouse, France



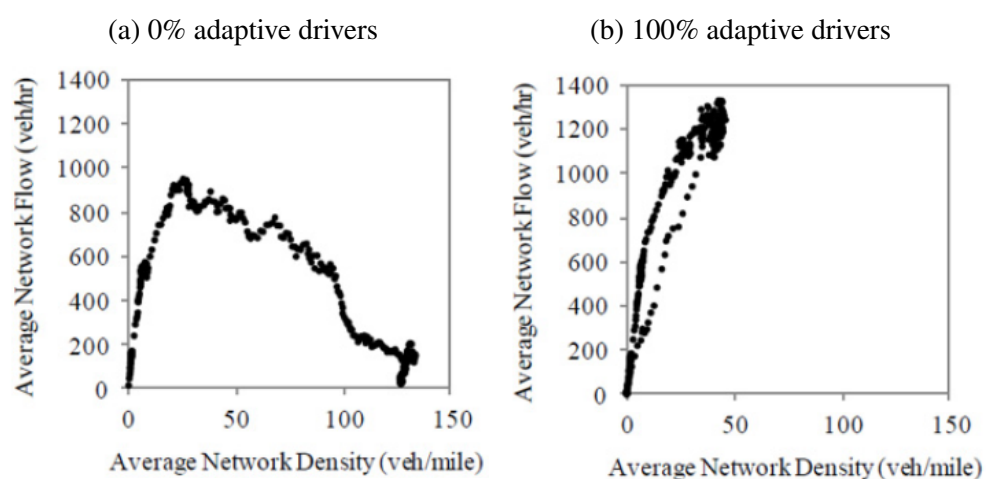
Source: (a) data: Geroliminis and Daganzo (2008), figure: Gayah and Daganzo (2011a); (b) (Buisson and Ladier, 2009)

The findings of Buisson and Ladier (2009) have generated much interest in explaining, characterizing and interpreting hysteresis loops, as well as in investigating the properties of a well-defined MFD. Gayah and Daganzo (2011a) revealed that hysteresis loops arise even under the most favorable conditions for an MFD and observed that a network's tendency towards unevenness is exacerbated during the last stages of a rush hour, causing hysteresis loops to perform a clockwise pattern. Geroliminis and Sun (2011) discovered by a comparison of flow and occupancy measures for an arterial network and a freeway network that an MFD is not well defined in

freeway networks as hysteresis effects are present. The authors also observed that the spatial distribution of vehicle density in the network is one of the key components that affect the scatter of an MFD and its shape, and that the different spatial distribution of congestion in freeway networks might explain the formation of hysteresis loops. This finding has been confirmed by Saberi and Mahmassani (2013) through the analysis of loop detector data from three different freeway networks within the United States. Based on empirical observation, the authors also characterize different hysteresis loops according to their size and shape.

The effect of adaptive driving in a network has also been subject of recent research. Gayah and Daganzo (2011a) state that when driver adaptivity is high, clockwise hysteresis loops are less likely to occur since a sufficient number of adaptive drivers balance congestion in a network during recovery. In an attempt to characterize gridlock and understand its dynamics, Mahmassani et al. (2013) found that the size of a gridlock (in terms of number of jammed links) shrinks as the population of adaptive drivers increases. When a sufficient proportion of drivers are adaptive, gridlock will eventually recover. Figure 4 shows the MFD for a network with no adaptive driving and a network in which all vehicles drive adaptively. When 100% of drivers are adaptive, the scatter and size of the hysteresis loop reduces and gridlock does not occur. Also note that the capacity of the network with 100% adaptive drivers is considerably higher.

Figure 4: MFD for different levels of adaptive driving

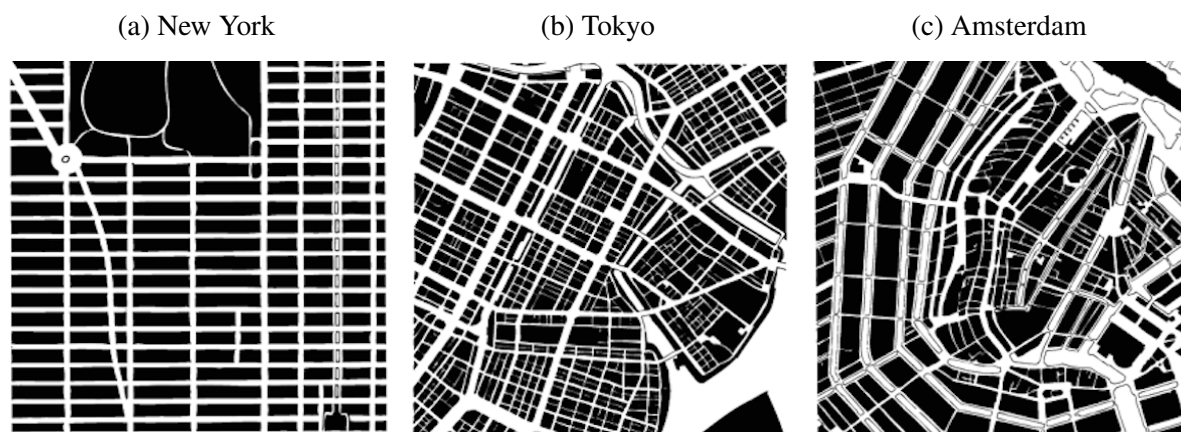


Source: Mahmassani et al. (2013)

## 1.2 Properties of urban networks

Urban street networks have a significant impact on the form and structure of cities. As Ortigosa and Menendez (2014) mentioned, the structure of a city (i.e. its urban pattern) has a prime role in the performance of traffic. Figure 5 illustrates the street network design of three global cities. The maps are drawn at the same scale and cover an area of approximately 2.6 km<sup>2</sup> (1 mi<sup>2</sup>). A wider selection of different street networks is provided in Appendix A.

Figure 5: Street network design of three global cities



Source: Jacobs (1993)

If we look at Fig. 5(a), showing the neighborhood of Manhattan in New York, we can observe a quite regular pattern in the street layout. This pattern could be described as grid, gridiron, rectangular, rectilinear, orthogonal or cellular, to name several examples. Even for this very simple street layout, there exists a variety of different classifications, which is one of the problems when trying to characterize network patterns. This is because no straightforward or standard descriptor exists to capture street patterns, as discussed by Marshall (2013). Also note that even very regular patterns such as the street network of Manhattan often contain irregular features, such as Broadway, which runs northwest to southeast through Manhattan. This leads to the question of generalization. Network models of real-world cities are always generalized to some extent, and the extent of generalization is usually subjective. In this particular case, one could argue to include Broadway as an essential feature of the Manhattan network pattern, but likewise for another purpose, Broadway could be excluded from the network model since it breaks up the New York grid. Both decisions can be justified depending on the purpose of the network model, but clearly the inclusion or exclusion of Broadway would lead to different results and findings.

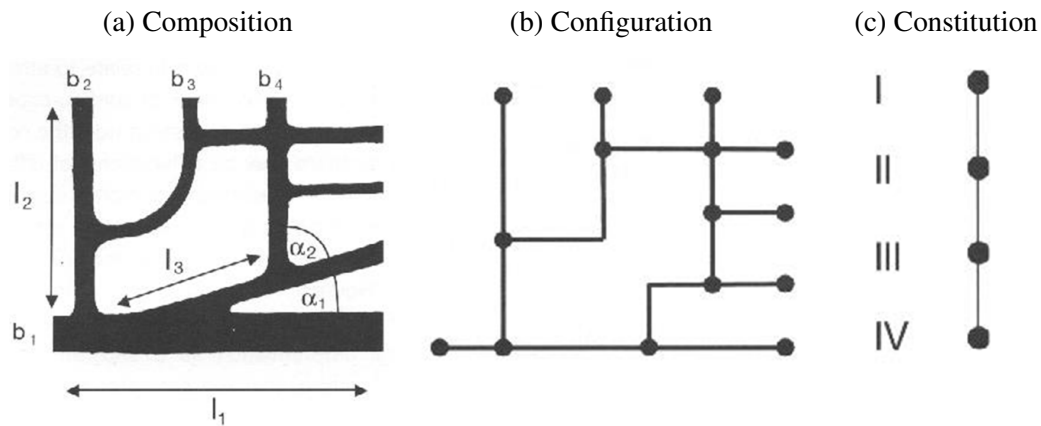
If we take a look at Fig. 5(b), showing a part of the Tokyo street network, we can observe another characteristic of urban street networks. Note that some of the streets in the network seem bigger than the surrounding streets. By isolating the bigger streets from the other streets of the network, one can observe that they seem to be part of a network on their own, creating an observable micro and macro structure within the network. Figure 5(b) therefore reveals different street classes and suggests some sort of street type hierarchy that seems to be present in urban street networks. This leads to the question of street classification. Just like networks, streets can be categorized in a whole spectrum of different types, e.g. according to street width, to traffic speed, to their strategic role in the network, or to the administrative unit that is in charge of building or maintaining the street. Besides determining the classification criterion, it is usually also necessary to determine the number of different classes within that criterion. As was the case for network patterns, there is no straightforward approach for the classification of the streets within a network and the classification criteria: The size of different classes will depend on the purpose of the modeled network.

Compared with the maps of Manhattan and Tokyo, the street network of Amsterdam shown in Fig. 5(c) is much harder to label. This is the case because Amsterdam includes a variety of different street patterns that evolved over time as the city grew. Note also that some parts of the illustrated network are easier to define than others. For instance at the top-left of the map, one can observe a rectangular grid that resembles the gridiron pattern of Manhattan. Next to the grid, one can observe a few main streets that enclose the city center following alongside the horse-shoe shaped canal system that very much forms the shape of the city of Amsterdam. The old-town itself contains a network pattern that is rather hard to describe and characterize, because of the lack of a contiguous pattern and because of its complexity and fine-grainedness. This reflects the fact that some parts of a city might have been planned and therefore often contain a contiguous observable pattern, while other areas might have evolved over time, alongside of the main market street for instance, without any particular centralized planning. In general, it can be seen that the scale of blocks and street patterns has become larger with time, and newer cities usually feature simpler and more regular patterns. However street patterns are not only related to the time period when the city was built, but also to geography, differing cultures, city functions or purposes, design or political philosophies, and to technological demands, as Jacobs (1993) described.

The discussed examples demonstrated some of the problems that might arise when trying to describe and characterize urban patterns, which is an essential step since this thesis aims to relate urban network patterns to traffic production. As has been shown, an urban street network could be described through a multiplicity of properties, such as topology, block length, street width, speed limit, number of hierarchical sub-networks, etc. Furthermore, each property can often be addressed through a variety of different terms, as was shown for the topology of Manhattan. In

order to clarify which properties of a network are described, Marshall (2013) proposes the use of an integrated framework that consists of three concepts which he refers to as composition, configuration and constitution. The three proposed concepts are schematically shown in Fig. 6.

Figure 6: Components of a street network



Source: Marshall (2013)

Composition is associated with the absolute physical geometry of a network and might include types such as rectangular, circular or triangular. The elements of composition have properties such as area, length or width. Configuration on the other hand describes the topology of a network, which is reduced to a set of links and nodes for this purpose. By looking at the configuration of a network, one can determine its continuity or connectivity. Constitution refers to the hierarchy of a network and is based on hierarchical properties such as tier or type.

The reference to one of the three concepts will make it easier to understand which properties of a network are actually compared and which components of a network were changed to create the different generic network types that will be introduced in Section 2.

### **1.3 Objective of this master thesis**

Although there has been considerable research in exploring the MFD, hysteresis loops and describing and characterizing network patterns, little research has explored the effects of different network patterns on the MFD and the formation of hysteresis loops. This thesis aims to fill this gap and attempts to identify and explain the effects of different idealized urban network patterns on their traffic performance and their ability to recover from congested conditions, by using the MFD and comparing the size of the hysteresis loop for the observed patterns.

The remainder of this thesis is organized as follows. Section 2 first describes the developed networks, their properties and the used methodology. Section 3 reveals the simulation results and the main findings that can be drawn from them. Section 4 provides a critical discussion of the results including limitations of this thesis and relates the findings to the context of transportation planning and urban planning in general. Finally, Section 5 summarizes the major finding of this thesis and provides suggestions for future research.

## **2 Methodology**

In this section, methods used in this work are shown. The explored patterns and their characteristics are described before the network performance is shown using the MFD, and the size and shape of the hysteresis loops for the explored patterns. Once the results are revealed, further analysis is carried out to understand the results in more detail.

### **2.1 Methodology**

In order to explore the effects of urban street networks on their traffic performance and their ability to recover from congested conditions, five different network patterns were derived and built into street networks within the micro simulation software Aimsun. For each pattern, ten simulations were run with ten different random seeds. A ‘random seed’ is a number used to initialize a pseudorandom number generator. The numbers obtained from the pseudorandom number generator are used in order to consider the stochasticity of the different parameters in micro simulation models (Menendez, 2013). For this reason, the results of each pattern are actually an average of the ten simulation runs carried out for each pattern. To obtain the needed output, different application programming interfaces (APIs) for Aimsun were written respectively already written APIs were modified to meet the needs of this thesis. For network analysis, the simulation output, which consists of the vehicle trajectories, was aggregated over time and space within the computing environment MATLAB.

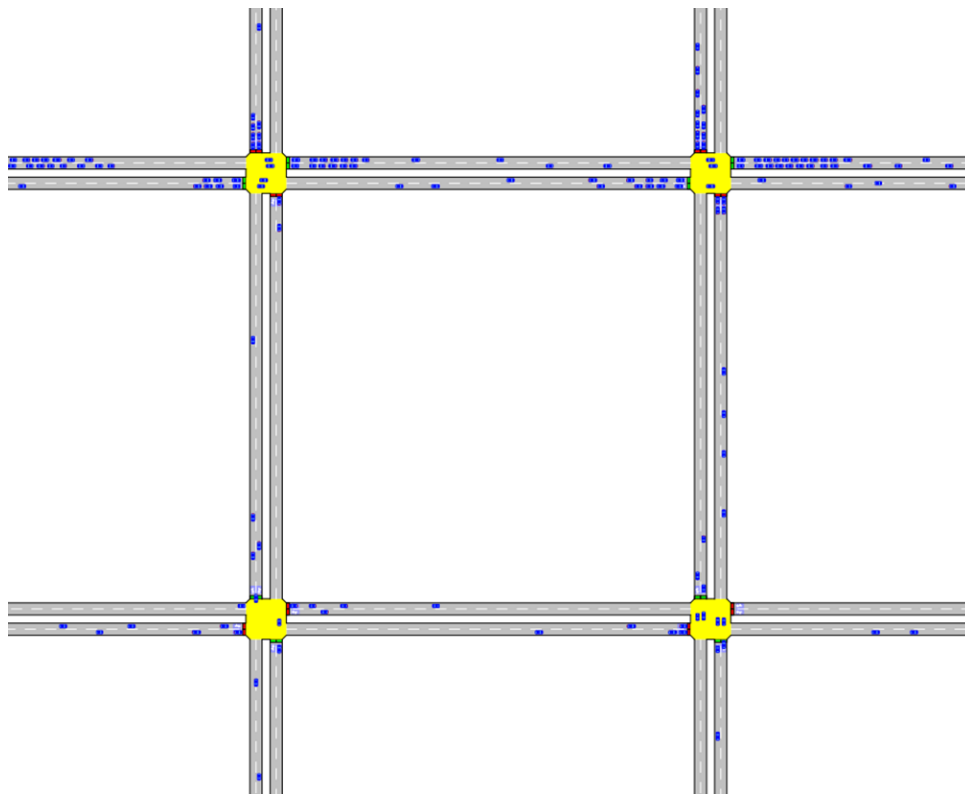
### **2.2 Micro simulation**

Microscopic traffic simulators are useful tools for designing, evaluating and optimizing transportation systems (Ge and Menendez, 2013). In a micro simulation, each vehicle moves in the network according to certain physical characteristics of the vehicle, the fundamental rules of motion and rules of driver behavior. This modeling approach differentiates microscopic simulations from macroscopic simulations, who simulate traffic flow by taking into consideration cumulative traffic stream characteristics and their relationships to each other (Menendez, 2013).

For this thesis, the traffic modeling software Aimsun was used. The decision to use Aimsun was mainly motivated because of its availability at The Pennsylvania State University where the work for this thesis was carried out and also because previous work with Aimsun at The Pennsylvania State University has resulted in a series of scripts and codes which have been very

useful for the development of this thesis, in particular for the generic construction of the network patterns described in Section 2.3. Nevertheless the author would hereby also like to thank PTV for their generous offer of a student license for the traffic modeling software Vissim. Figure 7 shows a portion of a network that was built within Aimsun.

Figure 7: Network screenshot from Aimsun



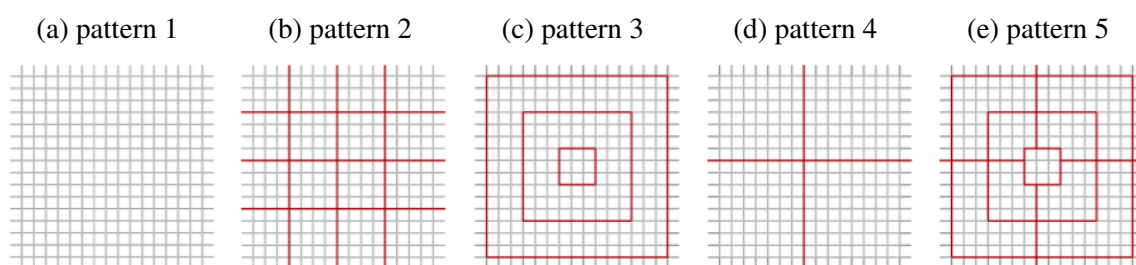
### 2.3 Patterns, intersection layout and signal phases

All networks except for pattern 1 consist of a local street network (micro structure) and an arterial street network (macro structure).

While the local street network was kept the same for all patterns and consists of a 16 x 16 grid with equal street lengths, the arterial street network was changed to represent five different idealized network patterns as illustrated in Fig. 8.

Considering the three concepts to classify street networks introduced in Section 1.2, the patterns are different from each other with regard to the configuration of the arterial network. The patterns are named as follows.

Figure 8: The five implemented patterns (red lines show arterial streets)



- pattern 1: basic grid (this pattern consists only of the local street network)
- pattern 2: grid within a grid
- pattern 3: rings
- pattern 4: radials
- pattern 5: ring and radials combined

The difference in street hierarchy (i.e. the difference in constitution) was implemented in two different ways. For this reason, for every pattern except for pattern 1 there exists a version A and version B, resulting in nine different networks overall. In all version A patterns, both local and arterial streets have two lanes per direction. In these A versions, arterials only differ from local streets in that their movement at intersections is prioritized through additional time for movement. For the version B patterns, in addition to more green time, all arterial streets consist of four lanes per direction, while local streets continue to have two lanes per direction, as illustrated in Fig. 9. Since all arterials are placed where otherwise a local street would be, this implies that the total network length in lane kilometers is the same for all A versions, but different for the B versions because of the added lanes on the arterials. Table 1 gives an overview of all explored patterns and their corresponding network length in lane-kilometers.

Table 1: Network length of the explored patterns in lane-kilometers

	1	2A	3A	4A	5A	2B	3B	4B	5B
local network	435.2	353.6	348.8	408	326.4	353.6	348.8	408	326.4
arterial network	0	81.6	86.4	27.2	108.8	163.2	172.8	54.4	217.6
total network length	435.2	435.2	435.2	435.2	435.2	516.8	521.6	462.4	544

For simplicity, signal controls always give a green time to the two opposing directions, while the other two directions have red during this time (two-phase traffic signals). Yellow time was set to three seconds for all intersection types, with a total interphase period of four seconds. The cycle length for the different intersection types illustrated in Fig. 9 were chosen as follows:

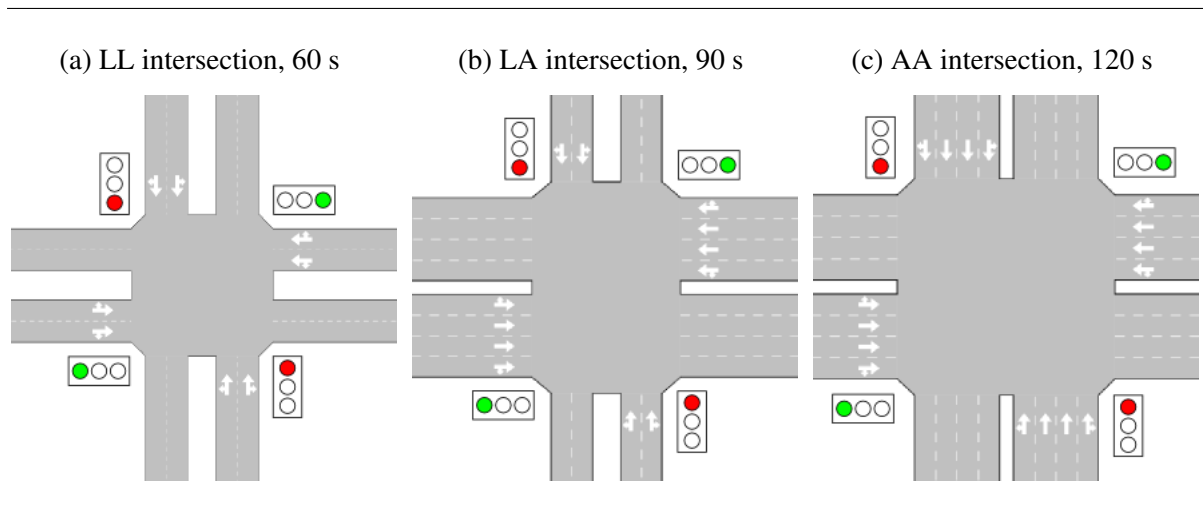
- Local street and local street: 60 s  
26 s green time for both approaches
- Local street and arterial street: 90 s  
26 s green time for local approach, 56 s green time for arterial approach
- Arterial street and arterial street: 120 s  
56 s green time for both arterial approaches

In all A patterns, every node consists of a four leg intersection with two lanes per leg (except for the cul-de-sacs at the periphery of each network). Each left (respectively right) turn is shared with a straight approach, as shown in Fig. 9(a).

In the version B patterns, there are three different types of intersections. The first one is the same as described above and occurs when a local street intersects with another local street (Fig. 9(a)). If a local street intersects with an arterial, the arterial has four lanes. At intersections, two out of those four lanes are through-only lanes, while the left and the right lane are shared lanes that allow both through and turning movements. (Fig. 9(b)). If an arterial intersects with another arterial, then all legs consist of four lanes (Fig. 9(c)).

Intersections are evenly distributed and spaced over a distance of 200 m. Each lane has a capacity of 1800 veh/h and a speed limit of 50 km/h. The different networks cover an area of roughly 13.7 km<sup>2</sup>, more than five times the size of the street networks shown in Fig. 5. The intersection layouts, the corresponding signal phases and the cycle lengths are illustrated in Fig. 9. Since in all version A networks, arterials have only two lanes per direction, the intersection layouts shown in Fig. 9(b) and Fig. 9(c) only occur in the version B networks. In all A version networks, all intersection types have the layout illustrated in Fig. 9(a).

Figure 9: Intersection layouts, signal phases and cycle lengths



## 2.4 Demand and routing

In all patterns, demand was assumed to be uniform and homogeneous. For this purpose, every node in the network (i.e. all intersections plus all cul-de-sacs of a network) serves as a cell for the origin-destination matrix (O-D matrix). All cells exchange the same amount of trips with all other cells, imitating a homogeneous demand distribution. The number of trips between nodes  $i$  and  $j$ ,  $T_{ij}$ , is:

$$T_{ij} = \tau, \text{ if } i \neq j \text{ or } T_{ij} = 0, \text{ if } i = j \quad (1)$$

Different levels of  $\tau$  (i.e. the number of trips exchanged between two nodes per hour) provide different levels of network demand. Simulation runs were carried out for three different levels imitating a low demand network ( $\tau = 0.3$ ), a network with medium demand ( $\tau = 0.45$ ) and a high demand network ( $\tau = 0.6$ ). However, since this thesis focuses on the effects of different urban street networks in congested conditions, all of the following results are derived from simulations that were run with the high demand level. Since all networks consist of 320 nodes and the loading phase is exactly one hour, approximately 61,000 vehicles are simulated in every simulation run. It should be noted that the value for the high demand network was still chosen arbitrarily by looking at the MFD and the shape and size of the hysteresis loops for different demand levels. A more elaborate attempt to choose a suitable demand level for a generic network can be found in Ortigosa and Menendez (2014).

The logit stochastic route choice model was used for route choice. The logit function is the most frequently used and thus the most theoretically analyzed function for mapping decision behavior in traffic networks (PTV, 2013). The logit function uses the choice probability  $P_k$  of a given

alternative path  $k$  that can be expressed as a function of the difference between the measured utilities on that path and all other alternative paths,

$$P_k = \frac{e^{v_k \theta}}{\sum_{l \in K_i} e^{v_l \theta}} \quad (2)$$

where  $P_k$  is the probability that path  $k$  is selected,  $v_k$  is the perceived utility for path  $k$ ,  $v_l$  is the utility for the alternative path  $l$ , and  $\theta$  is a sensitivity parameter that determines how strongly the distribution responds to utility differences.

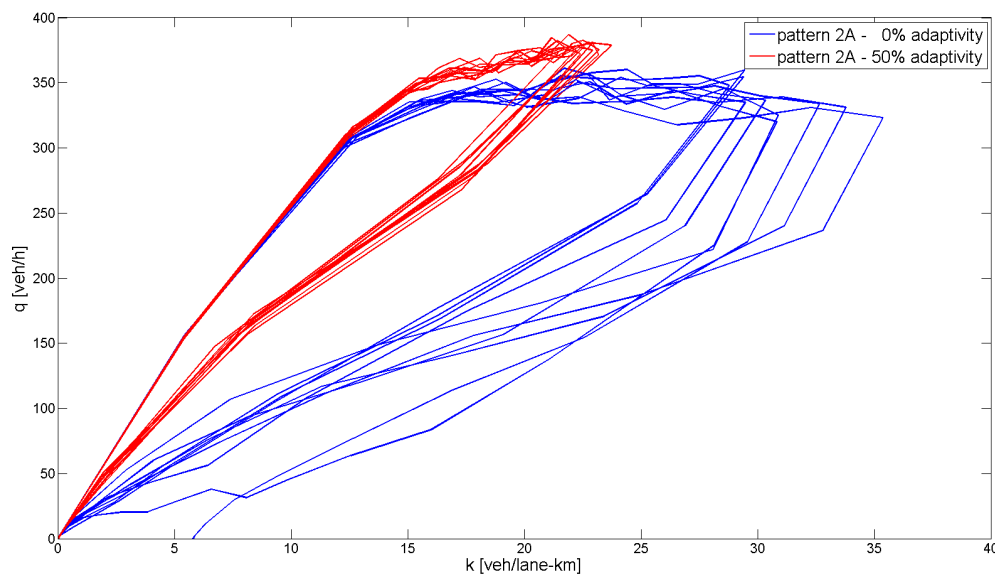
The cycle length that defines the time interval  $\Delta t$  used in the dynamic traffic assignment algorithm was set to 120 s. The total simulation time for each run is three hours, of which the first hour can be described as the ‘loading phase’ (i.e. trips are generated for all O-D relations according to the above mentioned demand levels) and the remaining two hours can be described as the ‘emptying phase’ (i.e. demand equals zero and the network has enough time to completely clear the networks of traffic).

## 2.5 Adaptive driving

First, simulation runs were carried out without adaptive driving. This means vehicles in the network cannot change their route while driving. Instead they strictly follow a path determined by the route choice algorithm described in Section 2.4 after entering the system. Evidently, this behavior is not realistic if some links in a network are fairly congested, given the network structure provides a variety of alternative routes to the drivers. In reality, it is highly realistic that drivers might alter their initial routes if they experience congestion en-route, especially if the drivers are familiar with the network structure. Besides the local drivers who are familiar with the network structure, adaptive drivers can also represent GPS-equipped vehicles that are capable of informing the driver about the network conditions. The effects of this so called ‘adaptive driving’ have also been subject to research. Gayah and Daganzo (2011a) discovered that instability in a network decreases if drivers adaptively re-route themselves and Mahmassani et al. (2013) observed that when a significant proportion of drivers are adaptive, gridlock will eventually recover.

In general, the inclusion of adaptive drivers provides more reasonable results. Figure 10 shows a comparison of the MFDs obtained for 10 simulation runs with different starting seeds for pattern 2A with and without the inclusion of adaptive driving.

Figure 10: Flow-density plots for different starting seeds of pattern 2A with and without adaptive driving



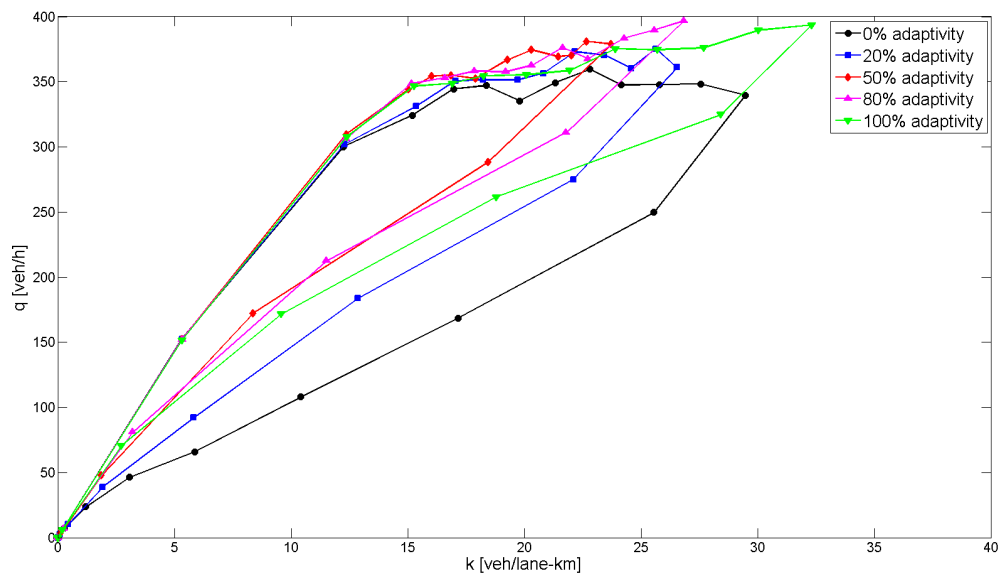
The inclusion of adaptive driving reduces the size of the hysteresis loop considerably and allows higher network flows. In addition, one of the the simulation runs without adaptive driving couldn't recover completely from congestion and a gridlock formed at a very low density of around six vehicles per lane-kilometer. While gridlocks in simulations can occur for such low densities, e.g., if all the streets around one single block get jammed, this behavior would hardly be expected in reality.

Another reason to include adaptive driving in this particular study is that the different arterial macro structures will provide various types of alternative routing that will influence how congestion in the network forms and how congestion dissipates. When comparing the different patterns, the inclusion of adaptive driving should therefore allow a more fair and realistic comparison.

To determine an appropriate value for the amount of adaptive drivers, simulation runs were carried out with different percentages of adaptivity. Results suggested that when approximately 50% of all vehicles in the network are allowed to drive adaptively, the networks perform the best, as illustrated in Fig. 11. For proportions of adaptive drivers greater than and less than about 50%, the size of the hysteresis loops appeared to increase, suggesting decreased network performance. This finding might be surprising at first and contradicts the findings made by Gayah and Daganzo (2011a) or Mahmassani et al. (2013). One possible explanation could be the way adaptive driving is implemented in the micro simulation used. The path selection for all

non-adaptive vehicles is made when a vehicle enters the system (initial assignment) according to the route choice algorithm. For the vehicles that are allowed to change their routes adaptively, this decision process is carried out again when new alternatives are available from the current position of the vehicle. Since the route choice model is carried out every cycle length  $\Delta t$ , some of the vehicles that are enabled to change their path will do this concurrently. The concurrent changing of route paths of many vehicles in the network might change the overall network traffic performance for the worse. For the aforementioned reasons and to increase the plausibility of the results, 50% of all vehicles in the network were allowed to drive adaptively, i.e., 50% of all vehicles can change their travel path en-route.

Figure 11: Different levels of adaptivity for pattern 2A



### 3 Results

For each pattern, ten simulations were run using different random seeds. After obtaining the aggregate results for each simulation run, one obtains information about the total travel distance, the total travel time, the average flow, the average density and the average speed for every five minutes of the simulation length (i.e. for every simulation interval).

Flow and density were calculated using Edie's generalized definitions:

$$q(A) = \frac{d(A)}{|A|}, \text{ and} \quad (3)$$

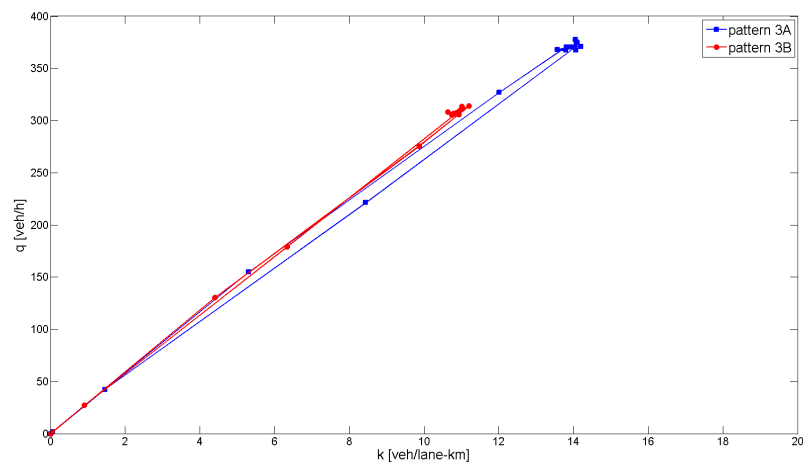
$$k(A) = \frac{t(A)}{|A|} \quad (4)$$

where  $A$  is a time-space region,  $|A|$  is used to denote the region's area,  $d(A)$  is the distance traveled in  $A$  and  $t(A)$  is the total time spent in  $A$  (Cassidy, 2003). The time-space region  $A = T \cdot dx$  is the region of temporal duration  $T$  and elemental spatial dimension  $dx$ , i.e. in this particular case the simulation interval and the length of the particular network, as shown in Table 1.

If the averages of the aggregated density vs. flow values for a particular pattern are plotted, the MFD for the network can be obtained. However, if versions A and B of a particular network are to be compared, the size and the shape of the MFD might be misleading since all the B versions have more lanes and therefore a bigger network length (measured in lane-kilometers), which is one of the two factors of the denominator of (3) and (4). Figure 12 shows the MFD for both versions of pattern 3 to illustrate this problem.

Note that the two MFDs shown in Fig. 12 seem to have the same basic shape, however the shape of the B version is considerably smaller than the A version even though the former has arterials that would be expected to increase the traffic network performance. Note especially that the maximum flow  $q_{max}$  of the B version seems to be much smaller than  $q_{max}$  of version A. This can be entirely explained by the fact that the total network length of the B version is considerably larger than the total network length of version A (since arterials in version B have four lanes per direction instead of two). Given the same demand and if looking at the flow in terms of vehicles per hour and lane-kilometer, it is expected that larger networks have lower flows for the same demand than smaller networks. However this should not mislead to the conclusion that the B

Figure 12: Flow-density plot of pattern 3



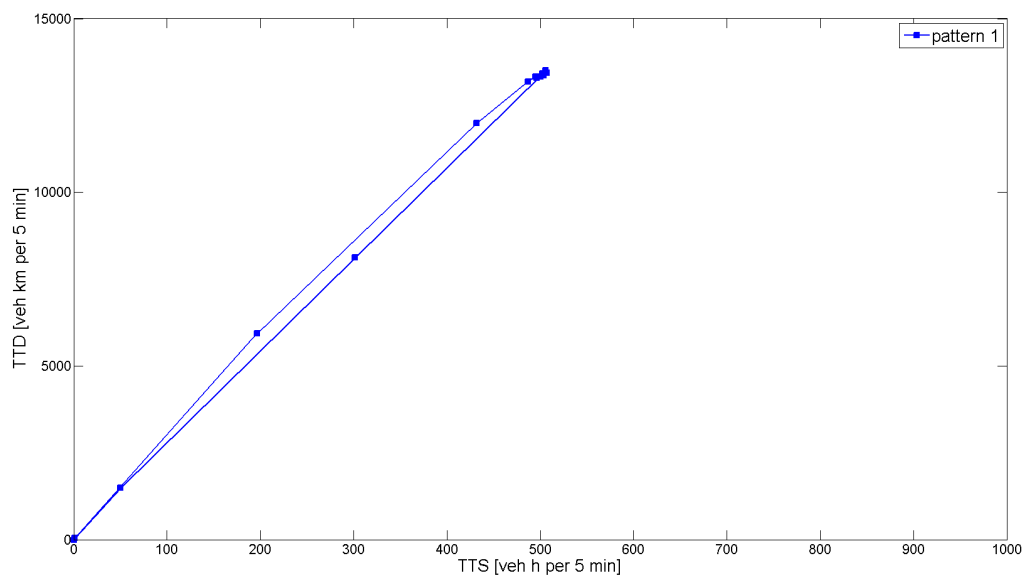
network is performing ‘worse’ than the A network.

To allow a more fair comparison between the two versions of the same pattern, network length (i.e. the spatial dimension  $dx$ ) was excluded from (3) and (4) and instead of plotting flow vs. density the total time spent (TTS in veh h per 5 minutes) and the total traveled distance (TTD in veh km per 5 minutes) for every simulation interval were used as proxies for  $q$  and  $k$  respectively. This approach is not uncommon practice and has been done in other studies as well, e.g. in Keyvan-Ekbatani et al. (2012)

### 3.1 Comparison within a specific pattern

In this section, for each pattern the version A network is compared to the version B network. The only exception to this is pattern 1, that doesn’t have any arterial streets. For pattern 1, only a small hysteresis loop can be observed. The network has not reached its capacity yet, pairs of values lie on a straight line with roughly constant positive slope, signifying that the network average speed doesn’t change during the loading phase. During the emptying phase, average network speed seems to be slightly smaller than during the loading phase, resulting in the formation of a clockwise hysteresis loop.

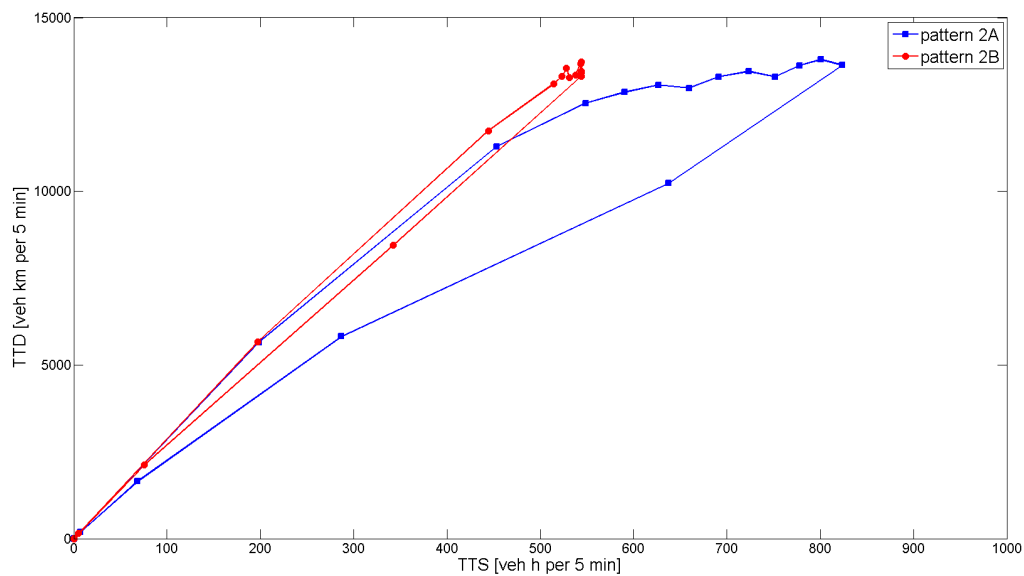
Figure 13: Time-space plot of pattern 1



For the 2A network shown in Fig. 14, a hysteresis loop of considerable size can be observed. The network seems to have reached its capacity and capacity flow sustains until the end of the loading phase. For the same amount of total traveled distance for every 5 min period, the total time spent in the network for every five minute increases. Speaking in terms of flow and density, this would mean that for the same flow, density increases with time until the end of the loading phase. However there is no decrease in flow (respectively total traveled distance) during this time. This means that the network as a whole is not jammed, but that some of the streets in the network suffer from congested conditions, resulting in a considerable decrease of the average network speed. Since demand drops to zero after the loading phase and remains there until the end of the simulation, the hysteresis loop closes at zero density and zero flow as there is no gridlock for this pattern for the given demand. If demand was not reduced to zero but just to a lower value than during the loading phase, the hysteresis loop would close at a point with higher density and flow (see Fig. 3(b) for comparison). Comparing the MFD of pattern 2A with pattern 1, it can be observed that pattern 2A, which includes an arterial network, performs worse than pattern 1, which only consists of the local street network. The conjecture for this behavior is that arterials provide less delay due to more green time at each signalized intersection along the arterial. Therefore, vehicles will tend to use the arterials disproportionately more than the local streets, resulting in uneven congestion. This effect (and others) will be discussed later in the document.

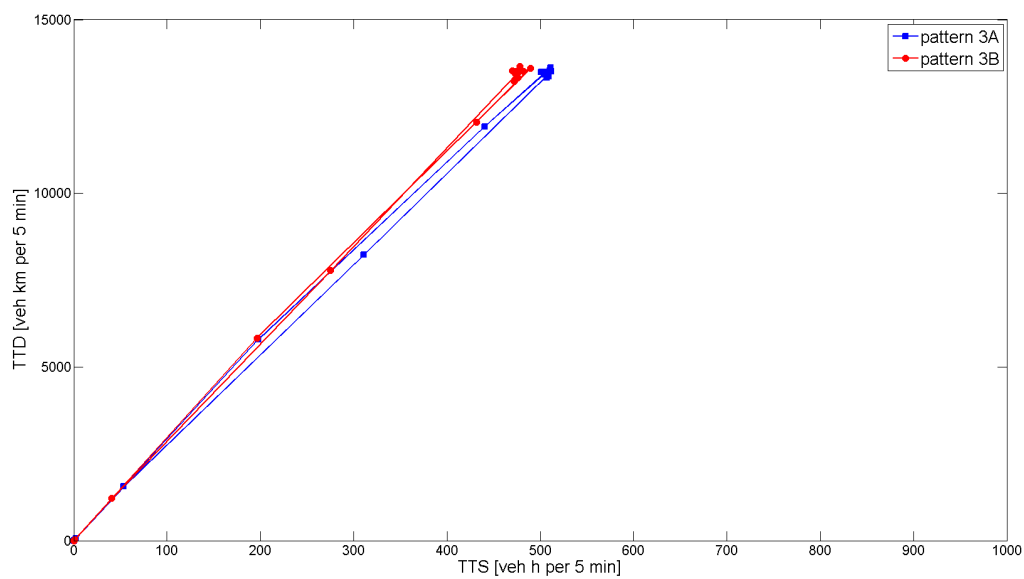
The hysteresis loop for network 2B on the other hand is much smaller and most points lie on a straight line with constant positive slope, reflecting almost no decrease in average network speed. Again it can be observed that for the same total travel time spent, total traveled distance is smaller during the emptying phase than during recovery phase. One reason why version B performs better than version A is that more capacity is provided on the arterial streets. Therefore, even though vehicles use the arterial network disproportionately more, the higher capacity in the B version of the networks mitigates the former effect.

Figure 14: Time-space plot of pattern 2



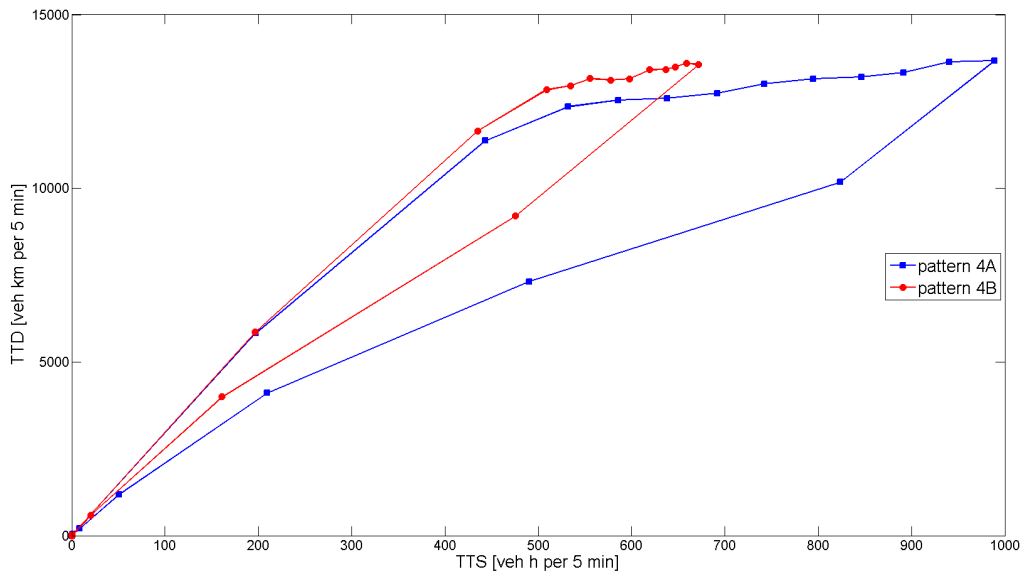
For pattern 3, two effects are immediately notable. First, that the difference between versions 3A and 3B is very small and second that all pairs of values of the simulation runs of both versions seem to lie on a straight line with constant positive slope, suggesting that both networks seem to be in free-flow condition for the entire duration of the simulation time. Average network speed for version 3A is a little bit higher than for version 3B, but the difference between the two networks is very moderate to the one observed for pattern 2.

Figure 15: Time-space plot of pattern 3



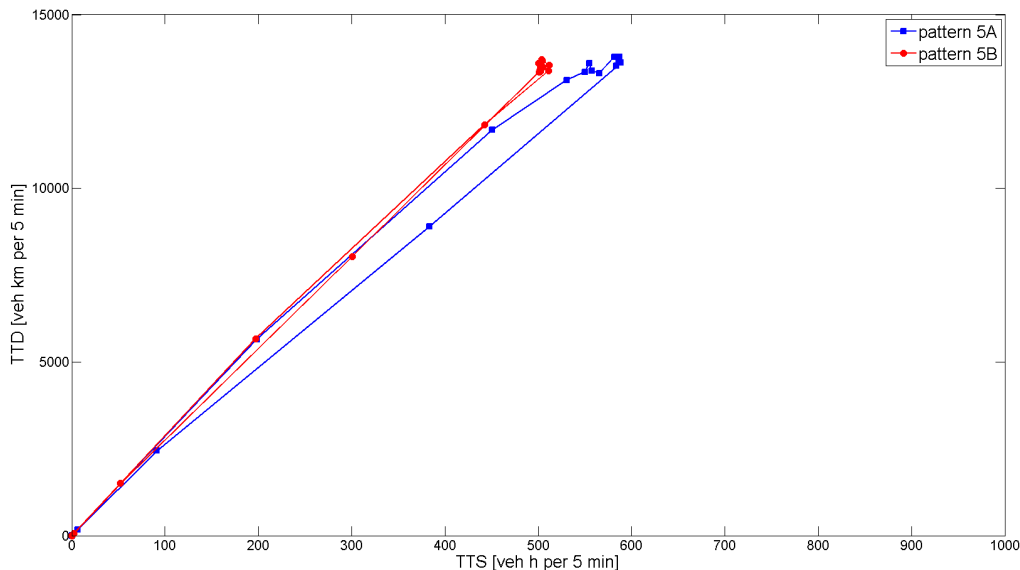
For both pattern 4A and 4B, noticeable hysteresis loops can be observed. Both network seem to reach capacity, however in pattern 4A average network speed decreases much more than in pattern 4B.

Figure 16: Time-space plot of pattern 4



For pattern 5A, the formation of a small clockwise hysteresis loop can be observed and average network speed seems to decrease before the network reaches its capacity. The value points for pattern 5B on the other hand seem all to lie on the free-flow branch of the MFD.

Figure 17: Time-space plot of pattern 5



As a general finding, it can be observed that for all patterns, the version B networks seem to perform better, resulting in higher average network speed. This is to be expected, since all B versions have a higher capacity on the arterials resulting in a longer network length in terms of lane kilometers. Furthermore it can be observed that for the same total travel time spent, total distance traveled is higher during the loading phase and smaller during the emptying phase, which confirms the findings made by Gayah and Daganzo (2011a) that networks are inherently more unstable as they recover from congestion than as they are loaded.

## **3.2 Comparison among different patterns**

After looking at each pattern individually, one can also compare the network performances among the different patterns. Figure 18 shows the MFDs for all A and B versions.

One can easily observe that the different network patterns perform differently and that there seems to be some kind of order that is mostly consistent for the A and B versions. Also one can easily note that the average size of the hysteresis loops is much smaller for the B version patterns than the A version patterns, as was already shown in Section 3.1.

By taking the size of the hysteresis loop and the average network speed obtained by the ration of flow to density as indicators for network performance, the different patterns can be ranked in terms of network performance from 'best' to 'worst'. For the version A patterns, pattern 3 seems to perform the best, followed by pattern 5, while pattern 2 and 4 perform the worst.

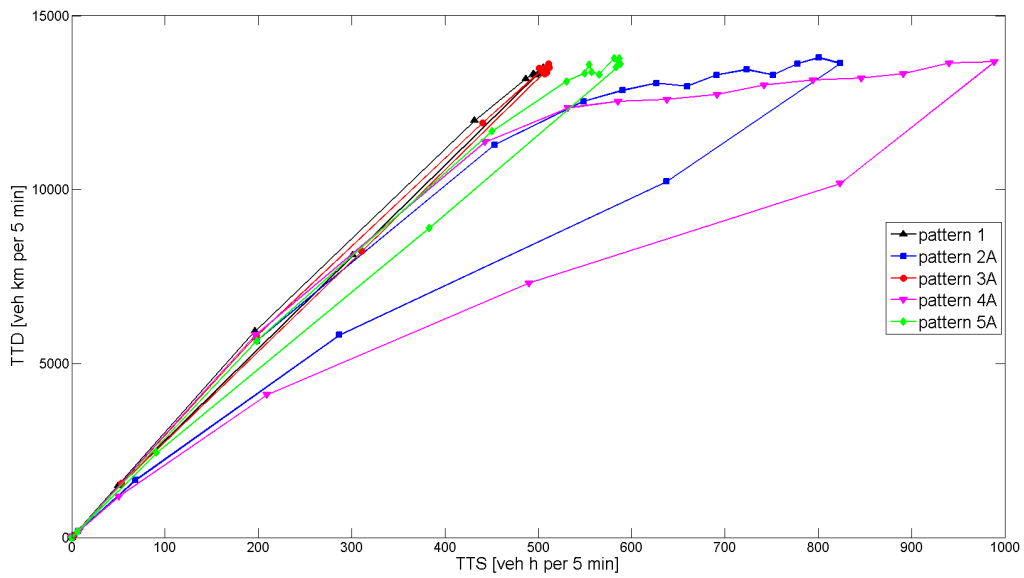
For the version B networks, pattern 3 shows the best network performance, followed by pattern 5, while patterns 2 and 4 perform the worst. Pattern 1's MFD is about equal to that of 3A respectively 5B with regard to its size and shape of the hysteresis loop.

Comparing patterns 2 and 4 with each other, i.e. the patterns that perform the worst, the A versions of patterns 2 and 4 seem to have a hysteresis loops of comparable sizes. While the size of the hysteresis loop for the version B of pattern 2 decreases considerably, this is not so much the case for pattern 4. The provision of more lanes to the arterial streets in this network seems to have a much smaller positive effect than for pattern 2 on the overall traffic performance. This is not surprising considering the much smaller arterial network in pattern 4, which results in a shorter overall network length (in terms of lane-kilometers) for 4B when compared to 2B (see Table 1).

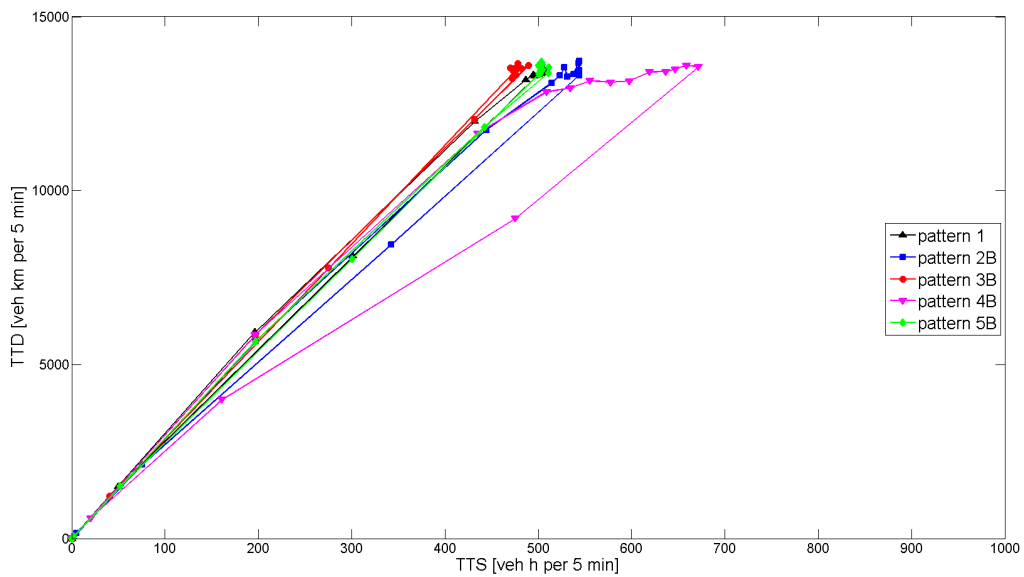
While the different performances of the patterns for the version B networks might be explained by their difference in the amount of arterial lane-kilometers provided, this does not explain the different performances for the A versions. In the following sections, further analysis is carried out in order to explore what properties might be responsible for the different performances of the different network patterns.

Figure 18: Time-space plot for all patterns

(a) version A networks



(b) version B networks



### **3.3 Impact of heterogeneity on traffic performance**

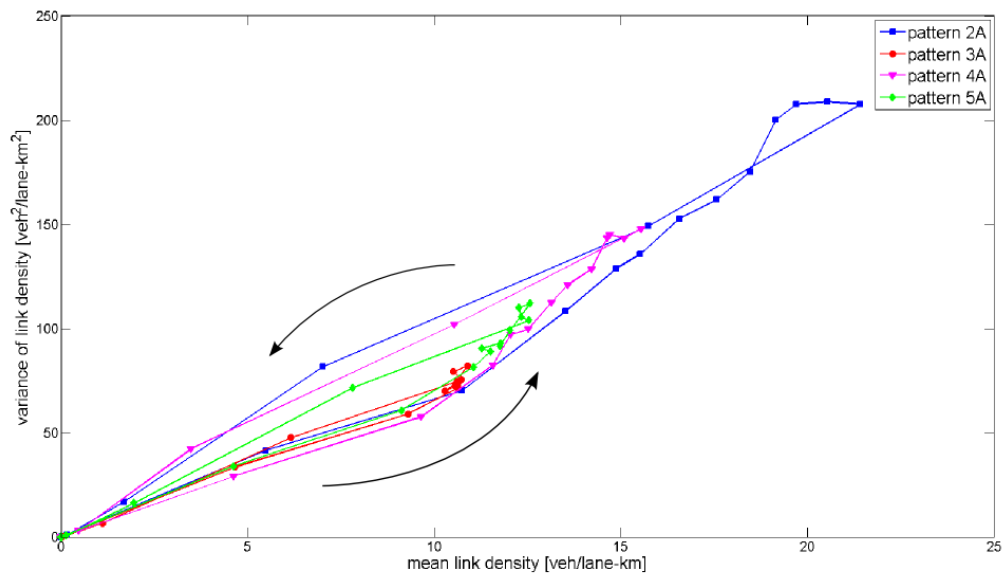
Previous research by Geroliminis and Sun (2011) has shown that a well-defined MFD with no hysteresis holds only for networks that are always homogeneously congested. The different performances of the explored network patterns and the formation of hysteresis loops with considerable size for some of them could therefore be explained to some extent by the heterogeneous spatial distribution of traffic and congestion in the networks. To test this assumption, for each pattern, the mean and variance of the densities for all links in a network were calculated for every five minutes. Figure 19 shows the line plot that results if one connects the data points for the variance of density [ $\text{veh}^2/\text{lane-km}^2$ ] among all links (y-axis) and the mean link density [ $\text{veh}/\text{lane-km}$ ] (x-axis) over time. The resulting line plots again reveal a hysteresis loop, however this time its formation is anti-clockwise. There seems to be a clear relationship between the mean of link density and the variance of link density. The higher the variance of the densities, the greater are the mean link densities and vice versa. This finding confirms the previous assumption, since a greater variance in link density is also an indicator for a more heterogeneous distribution of traffic in the network.

For the version A networks, pattern 2 and 4 have clearly the highest variance of link density. They also have the highest mean of link density and as shown in Section 3.2, patterns 2 and 4 also have the worst network performance.

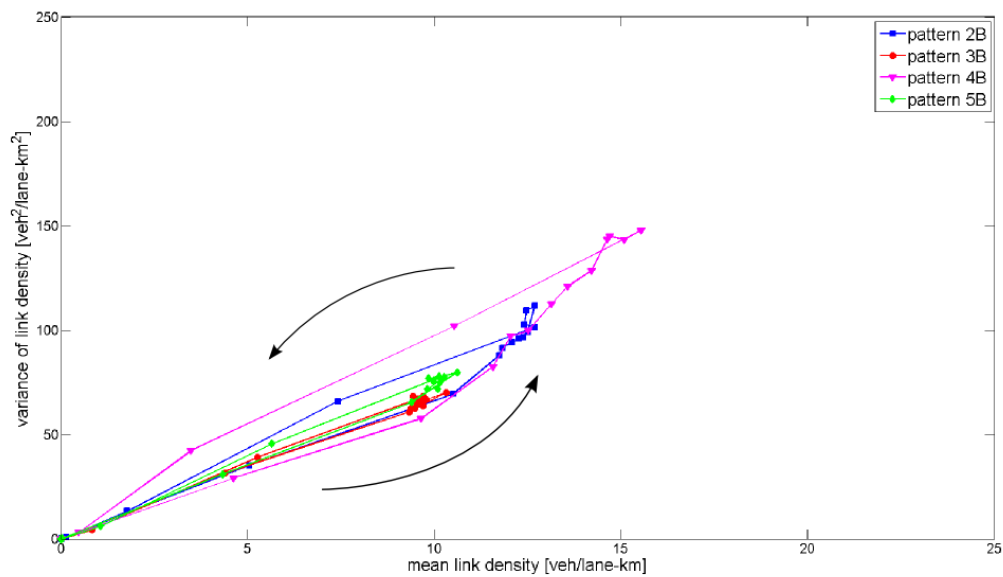
For the version B networks, pattern 4 has the highest variance of link density, followed by pattern 2, 5 and 3. Again this order matches the ranking of network performance for the different patterns as shown in Section 3.2.

Figure 19: Mean link density vs. variance of link density

(a) version A networks



(b) version B networks



### 3.4 Spatial distribution of congestion

We can further investigate the heterogeneous traffic distributions of the different patterns by looking at the spatial distribution of link density. Figure 20 shows all version A patterns including pattern 1. The pen-width of each link is an indicator of its link density. The larger the pen-width, the larger the mean link density on that link, with thresholds for link densities chosen at 20 veh/lane-km, 40 veh/lane-km and 60 veh/lane-km. The figure shows the link densities after one hour of simulation time, i.e. at the time when networks should have the most traffic. It can be clearly seen that pattern 2A and 4A are the networks with more links of high density than the other networks. As the demand and the network lengths are exactly the same for all patterns, this also means that the traffic distribution for patterns 2A and 4A is much more heterogeneous than the traffic distribution of the other patterns, with a lot of traffic on some of the links and almost no vehicles on the other links. Patterns 1, 3A and 5A on the other hand seem to have considerably fewer links with very high densities and therefore a more homogeneous distribution of traffic.

Figure 20: Spatial distribution of congestion for all A versions (red lines show arterial streets)

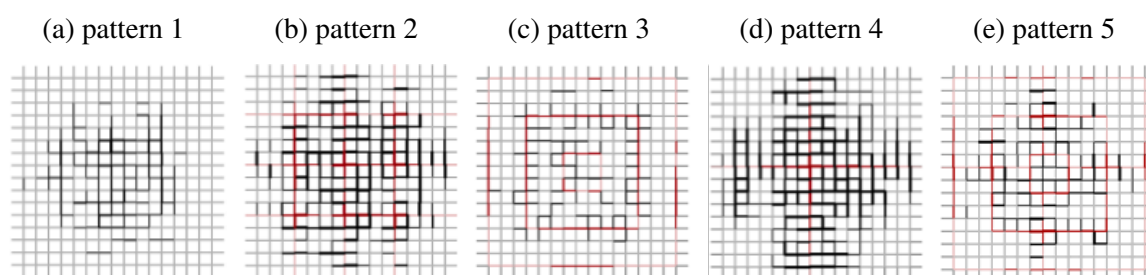
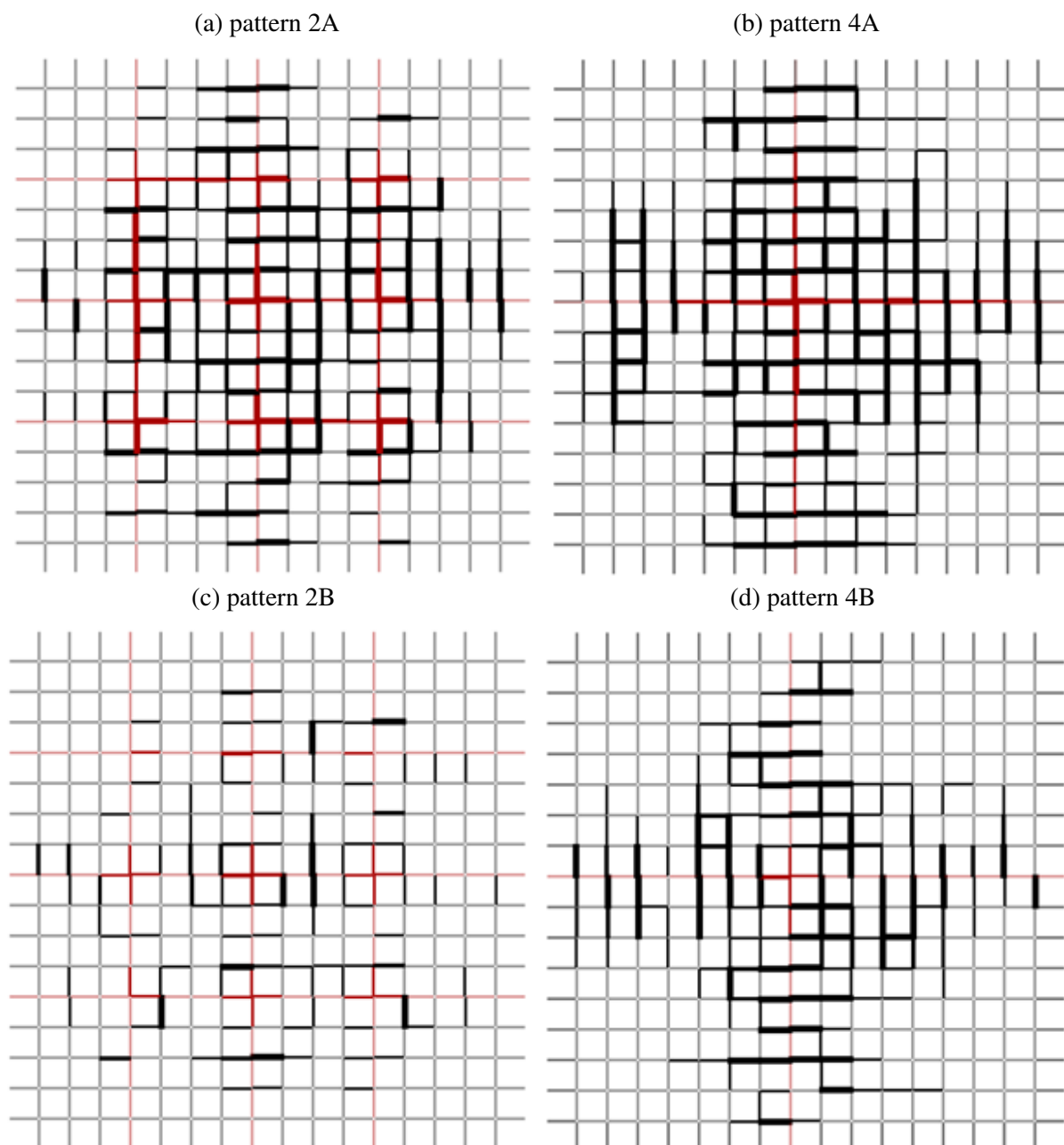


Figure 21 allows a more detailed look at the spatial distribution of link density for pattern 2 and 4, this time showing both versions of the two patterns. For both, patterns 2A and 4A, it can be observed that besides the arterial streets, the local streets directly connected to the arterials (so called ‘feeder links’ that allow vehicles to access the arterial) have very high densities. Some of the feeder streets seem to have enough traffic that they affect the local upstream streets connected to them. This seems especially to be the case in pattern 4A. It is also observable that in pattern 4A traffic seems to be mainly building up in the middle of the network around the central intersection of the arterial streets, while in the network of pattern 2A, traffic seems to be building up around the nine main intersections that connect an arterial street to another arterial street.

Figure 21: Spatial distribution of congestion for patterns 2 and 4 (red lines show arterial streets)



Although the network demand is exactly the same for the B versions, it is obvious that the amount of streets with higher densities is much smaller. This effect can be expected for all arterial streets, since they now have twice as much capacity. The increased capacity of the arterials benefits also the local street network. Note that the reduction of links with high densities between version A and version B seems to be larger for pattern 2. As discussed in Section 3.2, this can be explained by the difference in network length of the arterial network, which adds more than 80 lane-km to the B version of pattern 2, but less than 30 additional lane-km to the B version of pattern 4. Also note that the streets with high densities seem to be building up again

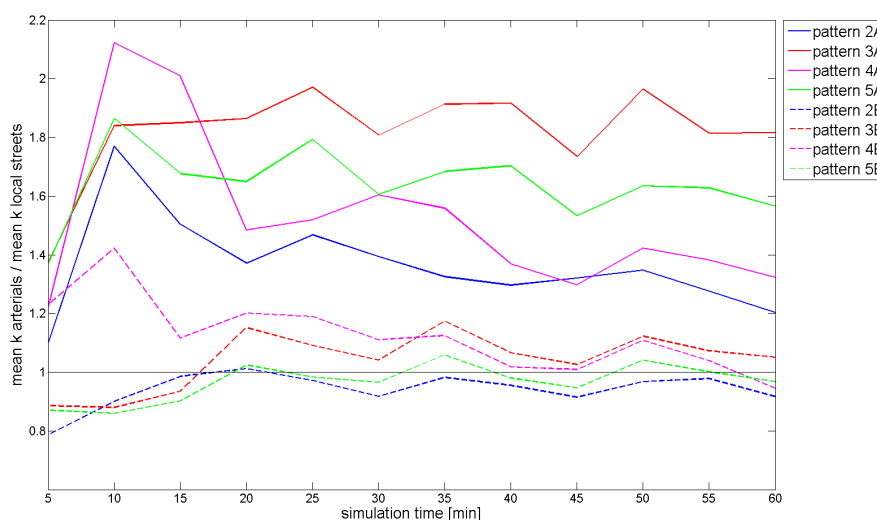
around the major intersections that connect arterials with arterials.

As has been shown, the local streets feeding the arterial streets and the arterial streets themselves seem to play an important role regarding the spatial distribution of traffic and the overall traffic performance of the network. For this reason, the role of the arterial streets and the role of local feeder streets in the network is explored in more detail in the following sections.

### 3.5 Arterial streets

Fig. 22 shows the ratio of the mean link density of all arterial streets over the mean link density of all local roads for all patterns, calculated per lane-kilometer. It can be observed that the mean link density on the arterials is much higher for all version A networks than for the corresponding B version networks, as already shown in Section 3.1. It can also be observed that for the A versions, patterns 2A and 4A have a high ratio at the start of the simulation, which decreases considerably during the length of a simulation. Patterns 3A and 5A on the other hand seem to have a more constant ratio over time. For the B versions, only pattern 4 has a ratio above 1 at the beginning. Just like pattern 4A, the ratio of pattern 4B decreases with increasing simulation length. The ratios for all other B version networks are very close to 1, i.e. arterial and local streets share about the same mean link density and the ratio stays stable for the entire simulation length. The instability of the ratios for patterns 2A, 4A and 4B could be an indicator of a more heterogeneous distribution of traffic in these networks. To further explore this assumption, the next section explores the traffic distribution on the local feeder streets.

Figure 22: Ratio of arterial street density to local street density



### 3.6 Local feeder streets

To explore the impact of the local feeder streets, each link within a network was grouped in one of the following categories: Local streets, local feeder streets, and arterial streets, as shown in Fig. 23 for pattern 2. For each street type, the mean link density per lane-kilometer was calculated.

Figure 23: Street types of pattern 2: local streets (green), local feeder streets (blue), arterial streets (red)

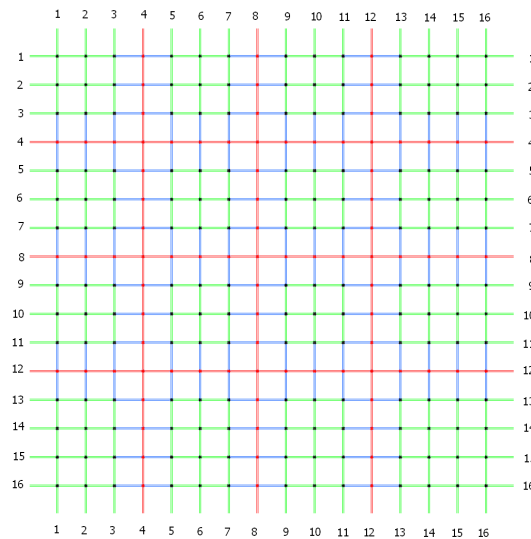


Figure 24 shows bar plots of the mean link density for the three distinguished street types of all version A patterns. Note that the class ‘all local streets’ also includes the local feeder streets. It is evident that in both patterns 2 and 4, local feeder streets have a considerably higher mean density than arterials, all local streets or all street types combined. The difference in mean link density is especially striking for pattern 4, with mean link density being about twice as high for local feeders than for the arterial streets. As was shown in Fig. 18, patterns 2 and 4 also have the worst network performance. Furthermore it can be observed that for all street types, the mean link density of patterns 2 and 4 are increasing during the loading phase (i.e. until 60 min of simulation time). Patterns 3A and 5A have the highest link densities on their arterial network, while the mean density of the local feeder streets is equal to the mean density of all local streets (pattern 3A) respectively only slightly higher (pattern 5A). Also note that after the initial loading phase (after around 10 min of simulation time) the levels of the mean link densities stay about the same until the end of the loading phase for patterns 3 and 5.

Figure 24: Mean link density for A versions: local streets (green), local feeder streets (blue), arterial streets (red), all streets (black)

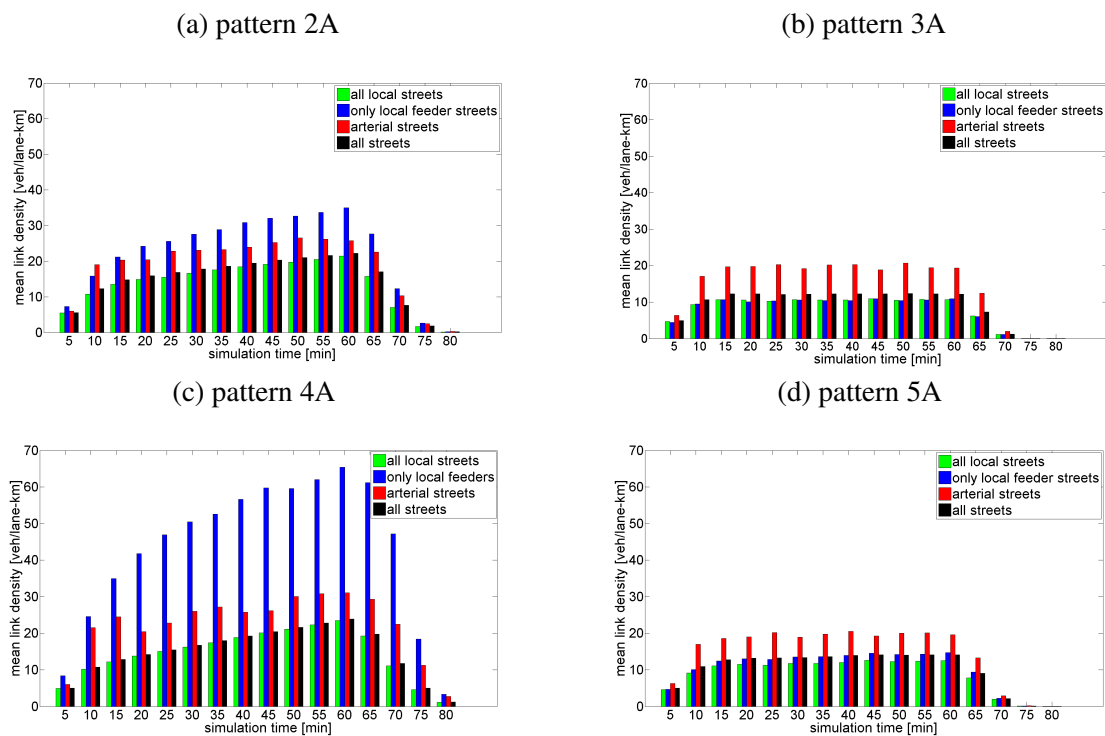


Table 2 shows the relative fractions of the network length in lane-kilometers for each street type of all A version networks. Again note that feeder streets are part of the local street network, so the percentages for the arterial and the local streets add up to 100%, while local feeder streets will always have a fraction smaller than all local streets since their network is a subset of the local streets network. In pattern 5A, arterials account for one fourth of the total network length in lane kilometers, the highest value of all A version networks. pattern 2A and 3A have about the same amount of arterials, while pattern 4A clearly has the lowest amount of arterials, with only 6% of the total network length. As the bar plots in Fig. 24 show, the mean link densities of patterns 2A and 3A are quite different, as is their network performance, although their arterial network length is very similar. Considering the fraction of local feeder streets, however, because of the different network structures there is a difference of more than 10% in network length. This finding suggests that not only the amount of arterials, but also their placement and the amount of local feeder streets affect the overall distribution of traffic in the network.

Looking at the mean link densities for the version B patterns in Fig. 24, there are a couple of things to notice. First, the mean link density of the arterials for the B versions are smaller than for the version A patterns, since in the version B networks the arterials have a larger capacity (four lanes instead of two lanes per direction). Note that all the densities were calculated per lane-kilometer, therefore the densities on the arterial streets can be compared with the mean link

Table 2: Fractions of the network length in lane-km for the different street types for all A versions

	pattern 2A	pattern 3A	pattern 4A	pattern 5A
local feeder streets [%]	29	40	11	42
all local streets [%]	81	80	94	75
arterial streets [%]	19	20	6	25

density for all other street types. Again patterns 2 and 4 have a higher mean link density on the local feeders than on the other explored street types. The densities of the different street types for patterns 3 and 5 are very similar, indicating a quite homogeneous distribution of traffic in the network, which results in the formation of a well-defined MFD. The densities for all street types except for local feeders are also for patterns 2B and 4B of roughly the same magnitude. If we compare version B with version A for patterns 2 and 4, it is observable that in pattern 2B the mean link density for all local feeders sustains around 20 veh/km for the entire simulation, while in pattern 2A, the mean density for local feeders increases during the loading phase. pattern 4 on the other hand shows an increase in mean link density during the loading phase for both, the A and the B version of the network pattern, reflecting the high amount of links with high densities previously found for pattern 4 in Fig. 21.

Figure 25: Mean link density for B versions: local streets (green), local feeder streets (blue), arterial streets (red), all streets (black)

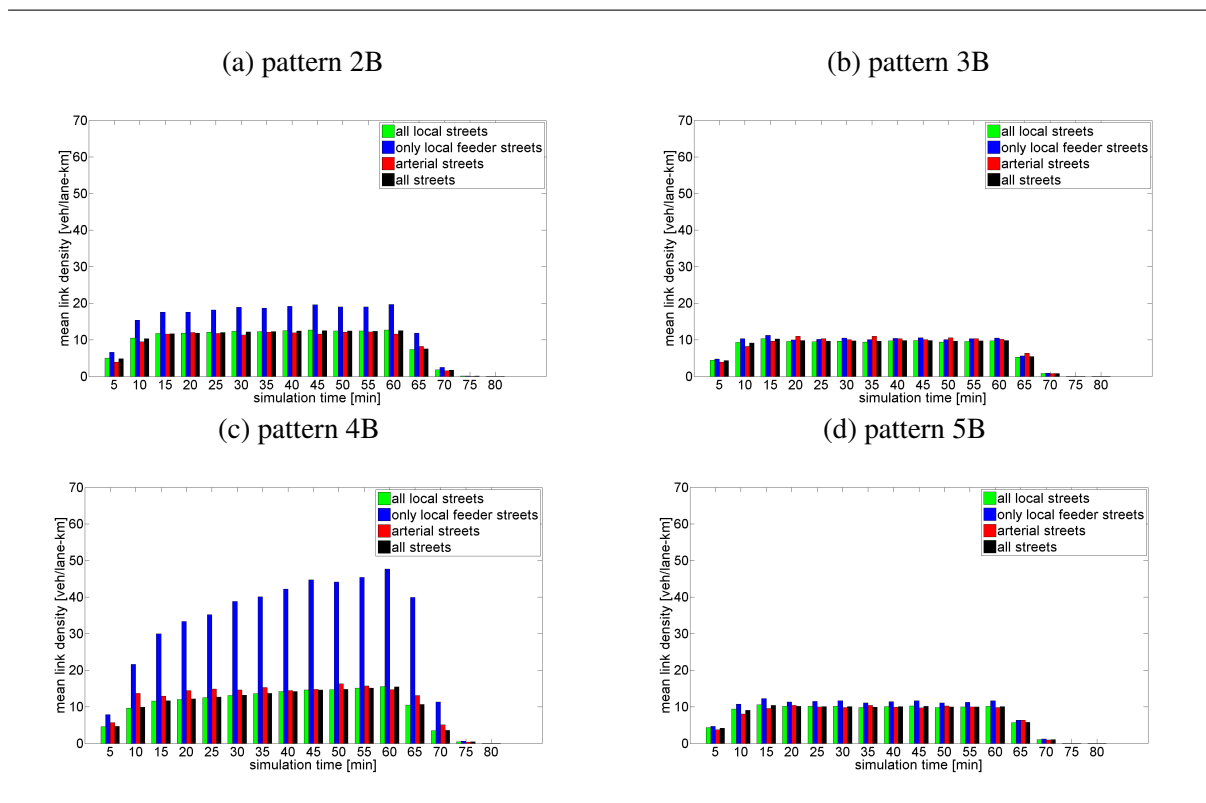


Table 3 shows the relative fraction of the network length in lane kilometers for each street type for all version B networks. Since the added capacity on the arterials in all version B networks affects the overall network length (see Table 1), the fractions of the network length of the street types differ from the A versions. Obviously, since every arterial now consists of two additional lanes, the fractions of the arterial streets increased, while the fraction of local streets and local feeder streets in the network decreased. The order of the fractions for the different patterns is still the same, however, the relative difference to each other has changed. In particular, this is the case with regard to the arterial streets. While in pattern 5B arterials account for almost half of the entire network length, in pattern 4B they make up just a little bit more than 10%. Also note that a higher percentage of arterial streets automatically means a larger network length in terms of lane-kilometers.

Table 3: Fractions of the network length in lane-km for the different street types for all B versions

	pattern 2B	pattern 3B	pattern 4B	pattern 5B
local feeder streets [%]	24	33	10	34
all local streets [%]	68	67	88	60
arterial streets [%]	32	33	12	40

In general, it can be said that the amount of arterials and local feeder streets in the networks seems to affect the network performance of the different patterns. The more arterials and local feeder streets, the lower are the mean densities and the better is the overall network performance. However, note that not all the differences in network performance can be explained by the amount of arterial or local feeder streets in a network. Although pattern 5 has the highest amount of both local feeder streets and arterials, pattern 3 actually has the best network performance, as was shown in Section 3.2. This is the case for both the version A and version B networks and suggests that not only the amount of arterials or local feeder streets, but also their placement in the network affects the overall traffic performance.

### 3.7 Turning maneuvers

As was shown, the provision of arterials and local feeder streets do affect the network performance, but they do not explain entirely the different network performances of the explored patterns. Studies suggest that turning maneuvers affect the stability of a network as well (Gayah and Daganzo (2011b), Daganzo et al. (2011)) and could therefore also potentially explain the different network performances. For this reason, the fraction and absolute amount of turning maneuvers was explored for all networks. Since all intersections have four legs, there are three

possible maneuvers for a vehicle from any approach: Turn left, turn right or go straight. The conjecture is that a higher value of left or right turns and a higher number of overall turning maneuvers causes more instability in a network and therefore leads to a worse traffic performance. Table 4 shows the percentages of the according turning type for all patterns.

Table 4: Turning maneuvers at intersections for all patterns

turning maneuver	1	2A	3A	4A	5A	2B	3B	4B	5B
left turn [%]	17	20	20	21	19	20	20	20	20
right turn [%]	18	21	19	20	20	17	17	18	17
straight [%]	65	59	61	59	61	63	63	62	63

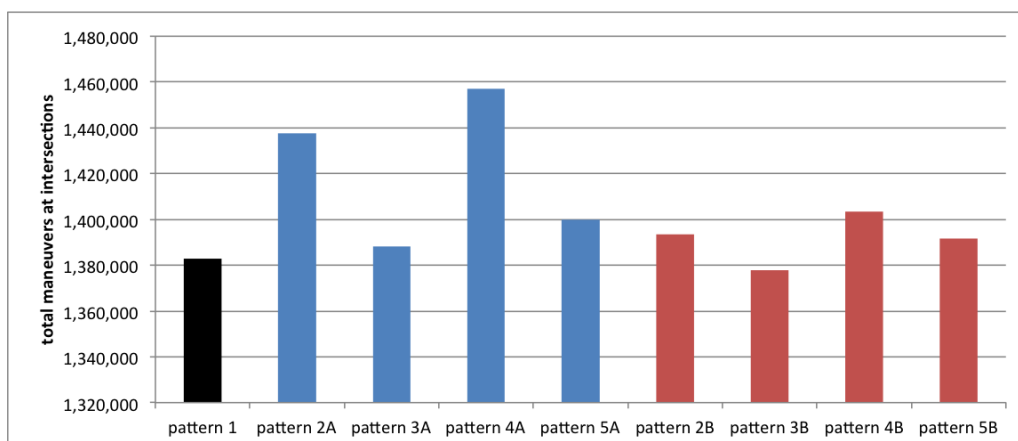
Although most of the values are very close to each other, there are some noticeable features. pattern 1 with no arterial network has clearly the highest fraction of vehicles moving straight. For all A patterns, the differences between left and right turn is never greater than one percent. Considering the relative fractions of vehicles moving straight, pattern 2A and 4A both have 59%, while patterns 3A and 5A both share a percentage of 61. Recall from ?? that patterns 2A and 4A have the worst network performance of all networks. Although the differences of the fractions of relative turning maneuvers are very small among the different patterns, there seems to be a relationship between the network performance and the vehicles going straight: The higher the fraction of vehicles going straight in a network, the better the traffic performance.

For the version B networks, considering the fraction of vehicles moving straight, patterns 2B, 3B and 5B have the same value, while pattern 4B has a value that is slightly smaller. Again, this correlates with the network performances of the B versions. Note that all version B networks have higher percentages of vehicles moving straight than their corresponding A versions, which is also related to the better traffic performance of the version B patterns.

Interestingly, all version B patterns have a higher relative amount of vehicles turning left than turning right, which is not the case for the A versions.

Figure 26 shows the total amount of maneuvers at intersections for all networks. Their order matches the ranking of the network performances shown in Section 3.2. The different network structures seem to affect the amount of turning, which leads to more or less stable networks and therefore differences in network performance.

Figure 26: Total maneuvers at intersections for all patterns



## **4 Discussion**

In this section, the findings made in the previous section are critically discussed and limitations of this work are shown. The findings are related to those of recent studies in this field of research and their significance on practical work in transportation engineering and urban planning are shown. Finally, possible directions of future research are shown and discussed.

### **4.1 Limitations and assumptions**

The networks built as part of this thesis are very simple and strongly idealized. It should be especially noted that the local network was kept the same for all network patterns. For the sake of simplicity, arterials were either given more priority at intersections (version A patterns) or in addition to that an increase in capacity (version B patterns). Other than that, they have the exact same attributes as the local street network. Of course, this is not very realistic, since one would assume that arterials would have a higher speed limit and a smaller intersection density for instance. In regard to the configuration of the different networks (i.e. their topology), it is important to note that the arterial streets can be described as a ‘superimposed’ sub-set of the local streets. This means that for a specific pattern, a certain link might be regarded as an arterial while in the other patterns the very same link is treated as a local street. If looking at the network as a whole, this implies that without distinguishing between local and arterial streets, all networks have exactly the same network configuration. Especially when trying to relate network performance with different network measures, future research should also consider networks that actually have a physical difference regarding their overall network pattern, i.e. they should have some difference in network configuration. With regard to composition, the only difference among the networks is the addition of lanes for the arterials of the version B patterns, resulting in a wider street width and differences in total network length in terms of lane kilometers. Other attributes of network composition, such as the angle or the orientation of the streets were kept the same for all patterns.

Another limitation of the network is the intersection layout. While the layout seems reasonable for the A version, the intersections of the B version networks that include an arterial street are not realistic as they do penalize any turning maneuver to a very high degree. A more realistic layout might include turn-only lanes for left and right turns. The control times for all patterns consist of a two-phase signal plan for all signals in the network. In urban networks, signal controls are usually not isolated but coordinated between multiple signals. This would at least be the case for the arterial street network.

Traffic demand is assumed to be homogeneous and was kept the same for the entire loading phase of the simulation. It is well known that traffic demand varies considerably throughout a day, such as morning and evening rush hour. The spatial distribution of traffic demand on the other hand can be very different from city to city and is of course strongly related to settlement structure and land use. Since all of the explored networks consist of a grid (if looking at the local street network), the assumption of a fairly homogeneous distribution of traffic demand seems reasonable. For networks with a different main structure, it might be necessary to introduce a demand that varies over space to match the specific urban structure.

A further limitation of this thesis is the classification of an urban network in just two different street types. This might be appropriate for some cases, but clearly the question about how many different street classes should be distinguished is of great importance and will lead to different results.

As has been described, network layout, traffic demand, intersection design and signal control were strongly simplified. However, this idealistic and simple approach also has some advantages. It is not the goal of this thesis to realistically describe the traffic flow of a city, but to explore the effects of urban patterns on a network's traffic performance. More complex and 'realistic' networks or simulation settings might not necessarily lead to better findings. The exploration of a very detailed network of a real-world city for instance might lead to results that are not generally applicable, and the inclusion of more factors and simulation parameters might make it harder to actually capture the effect of different network patterns on traffic. For this reason, the trade-off between the advantages and disadvantages of simple and generalized networks on the one hand and more detailed but also more specific networks on the other hand needs great care.

## **4.2 Main findings**

In Section 3, it was shown that different network patterns lead to different network performances considering network flow, density and speed. While this can be expected for networks with different network length as is the case for all B versions, different network performances were also observed for the version A networks with equal total network length, suggesting that the urban pattern does affect network performance. It was also shown that the version B networks have lower densities and overall higher network speed when compared to the A version networks, as can be assumed since the arterials in the B version have a larger capacity. For all networks a hysteresis loop can be observed, although shape and size of the hysteresis loops varies considerably among the different patterns. This confirms the finding made by Gayah and Daganzo (2011a), that networks are inherently more unstable as they recover from congestion

than as they are loaded. Furthermore, it was shown that networks with a high variance in link density also have a high mean link density. The existence of a well-defined relationship between variance of link density (respectively loop detector occupancy) and mean link density has also been shown by Geroliminis and Sun (2011). The effect of heterogeneity was further explored and the findings of previous research (e.g. Buisson and Ladier (2009) or Geroliminis and Sun (2011)) has been confirmed: The heterogeneity of spatial traffic distribution greatly affects network performance.

It seems to be that the heterogeneity of a network is at least to some part affected by the layout and the magnitude of different street types within that network, such as arterial streets and local feeder streets. The highest link densities of the patterns that showed the worst network traffic performance were observed on the local feeder streets. This also underlines the big impact of intersections in a network, since congestion on the local feeder streets were caused by the intersections that link the local street network to the arterial street network.

Both the fraction and the total amount of turning movements among the different networks were explored, since it is known that turning maneuvers affect the stability of a network. While the observed differences for the fractions of turning type (left turn, right turn and going straight) were very subtle, there seems to be a relationship between the fraction of turning maneuvers and network performance. The higher the fraction of straight movement for a network, the better the network performance. The differences of the total maneuvers at intersections for all patterns were more explicit and reveal again a relation to network performance. The higher the amount of maneuvers at intersections, the worse the network performance.

### **4.3 Practical significance**

Improved traffic management strategies such as congestion pricing, traffic metering or coordinated traffic signals can help to reduce congestion in urban areas and to use the existing infrastructure more efficiently. Such strategies could greatly benefit from information about the network wide traffic performance as provided by the MFD. Traffic management strategies should focus on reducing the size of the hysteresis loop, and vice versa, the size of the hysteresis loop can be used to monitor and assess introduced strategies. By gaining more insight about what factors contribute to the formation of hysteresis loops, adequate measures can be applied.

The founding of entire newly planned cities is rather rare, but not entirely uncommon, as the example of Masdar City in the United Arab Emirates proves. The extension of cities by newly built neighborhoods on the other hand is common in many places around the world. Urban planners could strongly benefit from more knowledge about the relationship between urban

structure and transportation in order to create more sustainable network structures.

However it is important to note that although the performance of different patterns allows some kind of ranking, this does not mean that the network structures that show a well-defined MFD should be necessarily preferred over patterns that show the formation of a large hysteresis loop for the same demand. The effects of urban patterns on transportation were only explored in regard to motorized individual transportation. Especially when dealing with urban areas, it is also necessary to investigate how network structure affects other modes of transportation, such as public transportation, pedestrians or bicyclists.

#### **4.4 Remaining questions for further research**

Further research could be directed in two different directions. There is need to explore the findings made in this thesis in more detail. For example, more attention could be directed to the effect of intersections, the role of turning and lane changing or the placement of the arterials in the network. More research is needed to better understand what exactly is causing more heterogeneous distributions in traffic networks and what measurements can be applied to mitigate these effects.

Research should also be directed towards a more integrated understanding of how urban patterns affect transportation, including other modes than just individual motorized traffic. With regard to transportation in urban areas, public transport and pedestrians should also be taken into account. Furthermore, it would be interesting to include a wider variety of idealized urban patterns and to validate if the findings of this thesis are also true for real-world networks.

## **5 Conclusion**

As part of this thesis, five different network patterns were built in a micro simulation environment to explore the effects of different network patterns on their traffic behaviour and ability to recover from congestion. Each pattern consisted of a local network that was kept the same for all patterns and an arterial network, imitating the micro and the macro structure of real-world networks. The difference in street hierarchy was implemented in two different ways: By prioritizing arterials at intersections through enhanced green times, and second, in addition to longer green times, by a bigger capacity on the arterial network. The traffic performances of the different networks were judged by the shape and size of the hysteresis loops.

The results of this thesis show that network patterns do affect the overall network traffic performance. Some of the findings made in recent studies were confirmed in this study. During recovery, the traffic distribution in the network seems to be more unstable than during the loading phase, resulting in the formation of hysteresis loops. It was also confirmed that the distribution of traffic in the network has a big effect on the network's traffic performance. Patterns that lead to a more heterogeneous traffic distribution usually are related with a bad traffic performance and not well-defined MFDs, while networks with a more homogeneous traffic distribution have well-defined MFDs. It was also found that both the magnitude and also the spatial placement of arterials in a network have a large impact on the overall traffic performance. Furthermore, a relationship between turning maneuvers and overall network performance was revealed. The lower the amount of total turning maneuvers and the higher the fraction of straight movements at intersections, the better is the network performance.

Future research should be directed to develop a more profound understanding of the factors contributing to heterogeneity in a network. For this reason it might be appropriate to explore a wider variety of idealized patterns and to validate the findings through real-world networks. Also, when exploring the relationship between streets and urban patterns, other modes of transportation such as public transport or pedestrians should be taken into account.

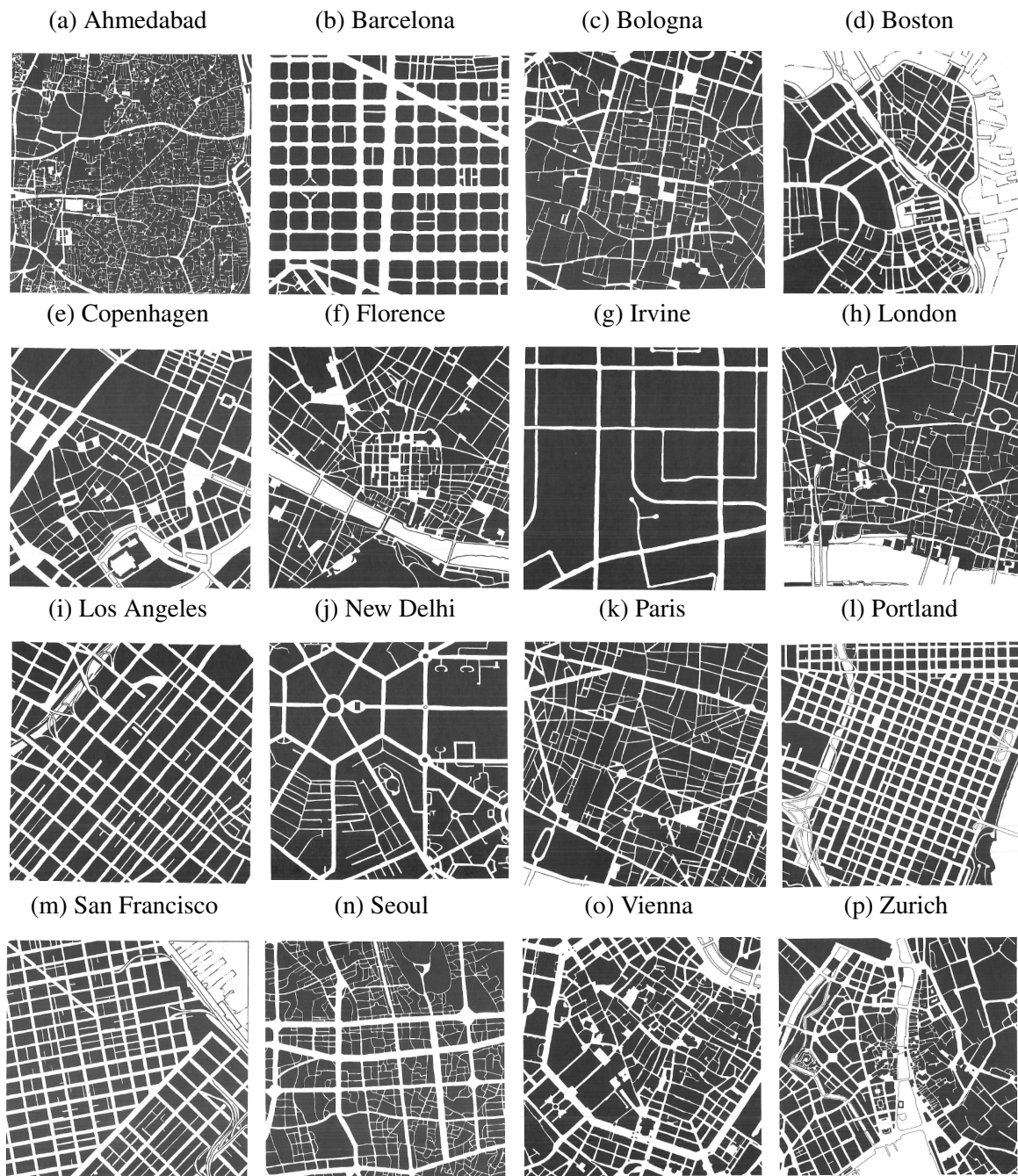
## 6 References

- Buisson, C. and C. Ladier (2009) Exploring the impact of homogeneity of traffic measurements on the existence of macroscopic fundamental diagrams, *Transportation Research Record: Journal of the Transportation Research Board*, **2124** (1) 127–136.
- Cassidy, M. J. (2003) Traffic flow and capacity, in *Handbook of Transportation Science*, Springer US.
- Cervero, R. (2002) Induced travel demand: Research design, empirical evidence, and normative policies, *Journal of Planning Literature*, **17** (1) 3–20.
- Daganzo, C. F. (2007) Urban gridlock: macroscopic modeling and mitigation approaches, *Transportation Research Part B: Methodological*, **41** (1) 49–62.
- Daganzo, C. F., V. V. Gayah and E. J. Gonzales (2011) Macroscopic relations of urban traffic variables: Bifurcations, multivaluedness and instability, *Transportation Research Part B: Methodological*, **45** (1) 278–288.
- Gayah, V. V. and C. F. Daganzo (2011a) Clockwise hysteresis loops in the macroscopic fundamental diagram: an effect of network instability, *Transportation Research Part B: Methodological*, **45** (4) 643–655.
- Gayah, V. V. and C. F. Daganzo (2011b) Effects of turning maneuvers and route choice on a simple network, *Transportation Research Record: Journal of the Transportation Research Board*, **2249** (1) 15–19.
- Ge, Q. and M. Menendez (2013) An improved approach for the sensitivity analysis of computationally expensive microscopic traffic models: a case study of the zurich network in vissim, paper presented at the *92th TRB Annual Meeting, Washington DC*.
- Geroliminis, N. and C. F. Daganzo (2007) Macroscopic modeling of traffic in cities, paper presented at the *Transportation Research Board 86th Annual Meeting*, no. 07-0413.
- Geroliminis, N. and C. F. Daganzo (2008) Existence of urban-scale macroscopic fundamental diagrams: Some experimental findings, *Transportation Research Part B: Methodological*, **42** (9) 759–770.
- Geroliminis, N. and J. Sun (2011) Properties of a well-defined macroscopic fundamental diagram for urban traffic, *Transportation Research Part B: Methodological*, **45** (3) 605–617.
- Godfrey, J. (1969) The mechanism of a road network, *Traffic Engineering and Control*, **8** (8).

- Herman, R. and I. Prigogine (1979) A two-fluid approach to town traffic, *Science*, **204** (4389) 148–151.
- Jacobs, A. B. (1993) *Great Streets*, MIT Press.
- Keyvan-Ekbatani, M., A. Kouvelas, I. Papamichail and M. Papageorgiou (2012) Exploiting the fundamental diagram of urban networks for feedback-based gating, *Transportation Research Part B: Methodological*, **46** (10) 1393–1403.
- Mahmassani, H. S., M. Saberi et al. (2013) Urban network gridlock: Theory, characteristics, and dynamics, *Procedia-Social and Behavioral Sciences*, **80**, 79–98.
- Marshall, S. (2013) *Streets and patterns*, Routledge.
- Martine, G. and M. Alex (2007) State of world population 2007: unleashing the potential of urban growth.
- Menendez, M. (2013) Introduction to traffic flow simulation (lecture notes).
- Menendez, M. (2014) Road transport systems (lecture notes).
- Ortigosa, J. and M. Menendez (2014) Traffic performance on quasi-grid urban structures, *Cities*, **36**, 18–27.
- PTV (2013) *PTV Vissim 6 User Manual*, PTV AG, Karlsruhe.
- Saberi, M. and H. S. Mahmassani (2013) Empirical characterization and interpretation of hysteresis and capacity drop phenomena in freeway networks, *Transportation Research Record: Journal of the Transportation Research Board, Transportation Research Board of the National Academies, Washington, DC*.

## A Selection of urban network patterns

Figure 27: Selection of urban network patterns, all drawn at the same scale



Source: Jacobs (1993)